# Extending Application of Simple for Dead and Continuous for Live Load Steel Bridge System to ABC Applications in Seismic Regions- Phase II- Experimental

Submitted by
Amir Sadeghnejad

PROGRESS REPORT
Period ending December 30, 2017

Department of Civil and Environmental Engineering
Florida International University
Miami, Florida



Submitted to
Atorod Azizinamini
Director, ABC-UTC
October 2017
**ABC-UTC**

# Contents

# 1. Introduction

The steel bridge system referred to as Simple for Dead load and Continuous for Live load (SDCL) has gained popularity in non-seismic areas of the country. Accordingly, it results in many advantages including enhanced service life and lower inspection and maintenance costs as compared to conventional steel systems. The main objective of this research was to extend the application of SDCL to seismic areas. The concept of the SDCL system was developed at the University of Nebraska-Lincoln and a complete summary of the research is provided in five AISC Engineering Journal papers. The SDCL system is providing steel bridges with new horizons and opportunities for developing economical bridge systems, especially in cases for which accelerating the construction process is a priority. The SDCL steel bridge system also provides an attractive alternative for use in seismic areas.

The SDCL concept for seismic areas needed a suitable connection between the girder and pier. In this research, an integral SDCL bridge system was considered for further investigation. The structural behavior and force resistance mechanism of the proposed seismic detail considered through analytical study in Phase I of this research. The followings are some of the finding of this phase (numerical and analytical study) that proposed a detail for SDCL for seismic zones.

The proposed connection (Figure 1-1) evaluated under push-up, push-down, inverse, and axial loading to find the sequence of failure modes. The global and local behavior of the system under push-down forces was mainly similar to non-seismic detail. The nonlinear time history analysis indicated that there is a high probability that bottom flange sustains tension forces under seismic events. The finite element model subjected to push-up forces to simulate the response of the system under the vertical component of seismic loads. However, the demand-capacity ratio was low for vertical excitation of seismic loads. Besides finite element results showed that continuity of bottom flange increased ductility and capacity of the system. While the bottom flange was not continuous, tie bars helped the system to increase the ultimate moment capacity. To model the longitudinal effect of earthquake loads, the model subjected under inverse forces as well as axial forces at one end. In this case, dowel bars were most critical elements of the system. Finite element analyses performed to investigate the role of each component of preliminary and revised detail. All the results demonstrated that continuity of the bottom flange, bolts area (in the preliminary detail), tie bars over the bottom flange (in the revised detail) were not able to provide more moment capacity for the system. The only component increased the moment capacity was dowel bars. In fact, increasing the volume ratio of dowel bars could be able to increase the moment capacity and prevent premature failure of the system.

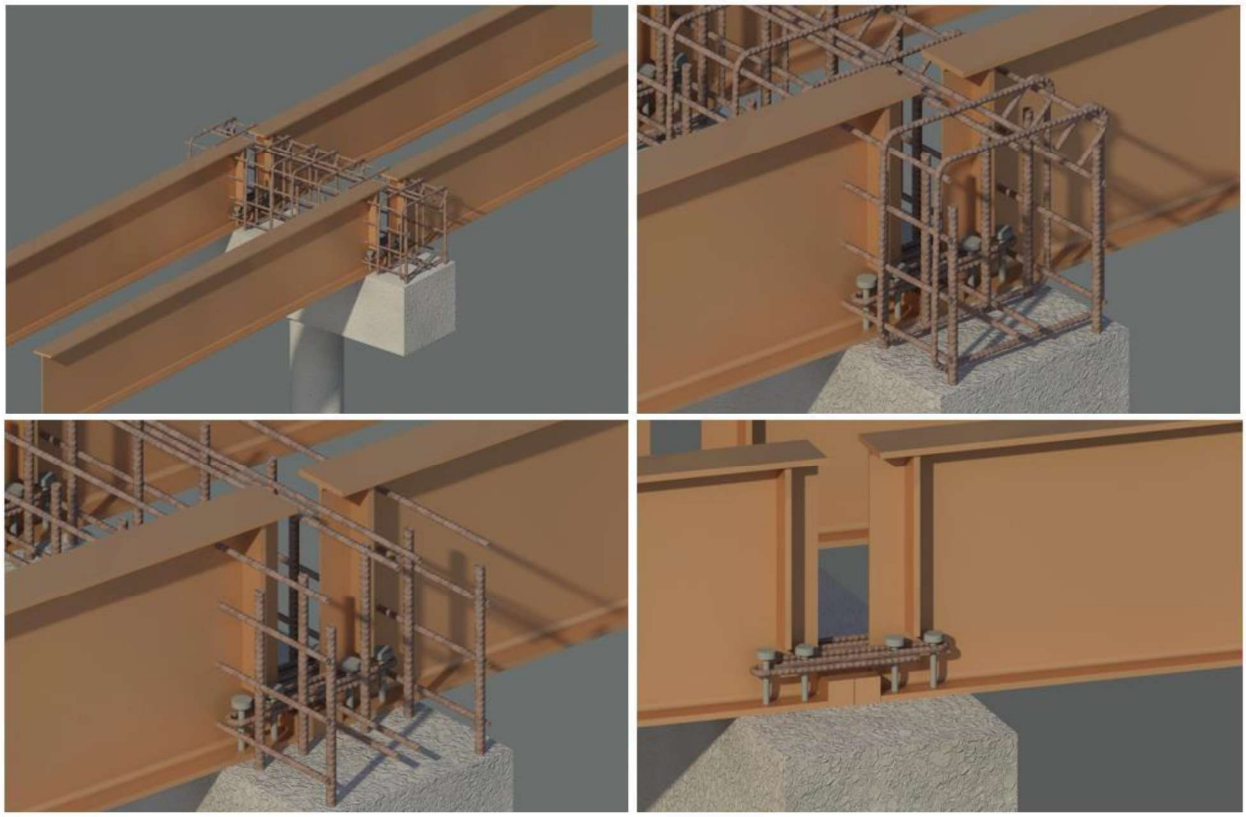

*Figure 1-1 Proposed connection by the Phase I of this research.*

Phase I of this research concentrated on developing suitable details mainly through numerical analysis and provided a comprehensive numerical study for the design of SDCL detail in steel bridges. In Phase II (current phase) of this research project, an experimental test will be conducted as a proof of concept test and evaluate the validity of the design recommendations. In the phase III of this project, a scale model bridge containing the SDCL detail will be subjected to a shake table test at the University of Nevada-Reno.

The following section describes the component test details of the one-third scale specimen and test setup used for evaluating the behavior of the proposed system under cyclic lateral loading to simulate the longitudinal component of the seismic loads.

# 2. Objectives

The main objective of the proposed project is design and verification testing of a component level specimen using a SDCL for seismic connection. During Phase I of the project, suitable details were developed using numerical analysis. The next step is performing component level testing on the connection details prior to a large scale shake table test. The goal of the component test is to proof load the connection between the substructure and superstructure. If designed properly, the failure should not occur within the connection itself. The objective of the proposed project is the design and testing of the component level specimen. This testing is being performed as a verification test

prior to shake table testing. The goal of the component test is to proof load the connection between the substructure and superstructure.

# 3. Component Test Details

An experimental testing program, capable of verifying the project recommendation in Phase II of the study was developed. A prototype two-span steel I-girder bridge was selected for finding the demand side of the detail over the pier under seismic loads. The prototype bridge was designed and scaled down to 1/3 for the purpose of Phase II and III of this research. The scaled down bridge was designed to undergo the same stresses as the prototype bridge. For the component testing, a column with two girders at two side considered to be constructed in the structure lab of FIU (Figure 3-1). Figure 3-2 to Figure 3-6 show the details of the constructed test specimen.

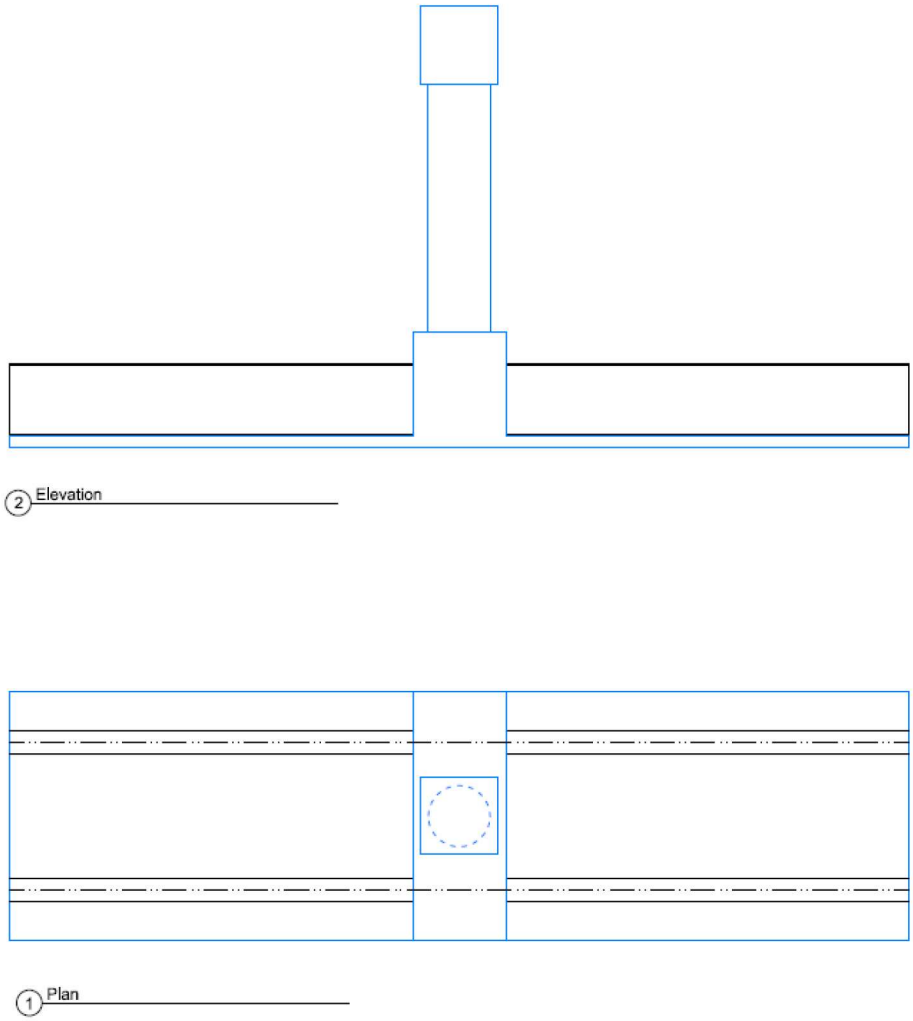


*Figure 3-1 Schematic view of the test specimen at FIU.*

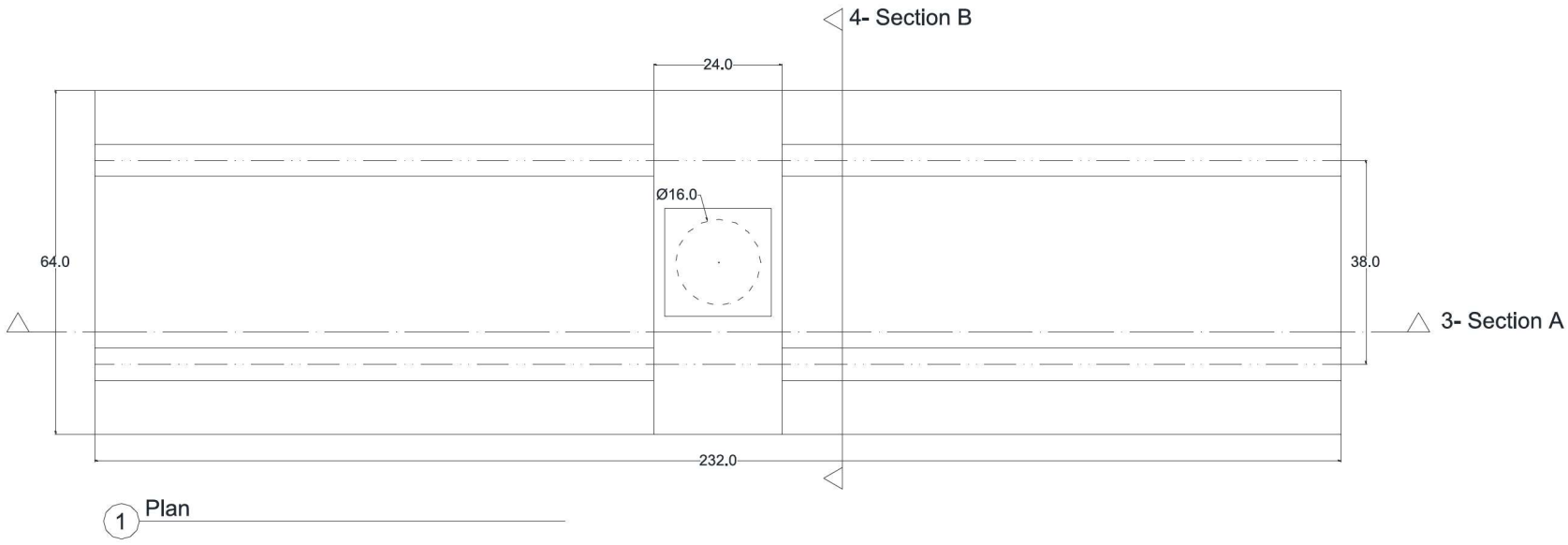


*Figure 3-2 Test specimen plan*

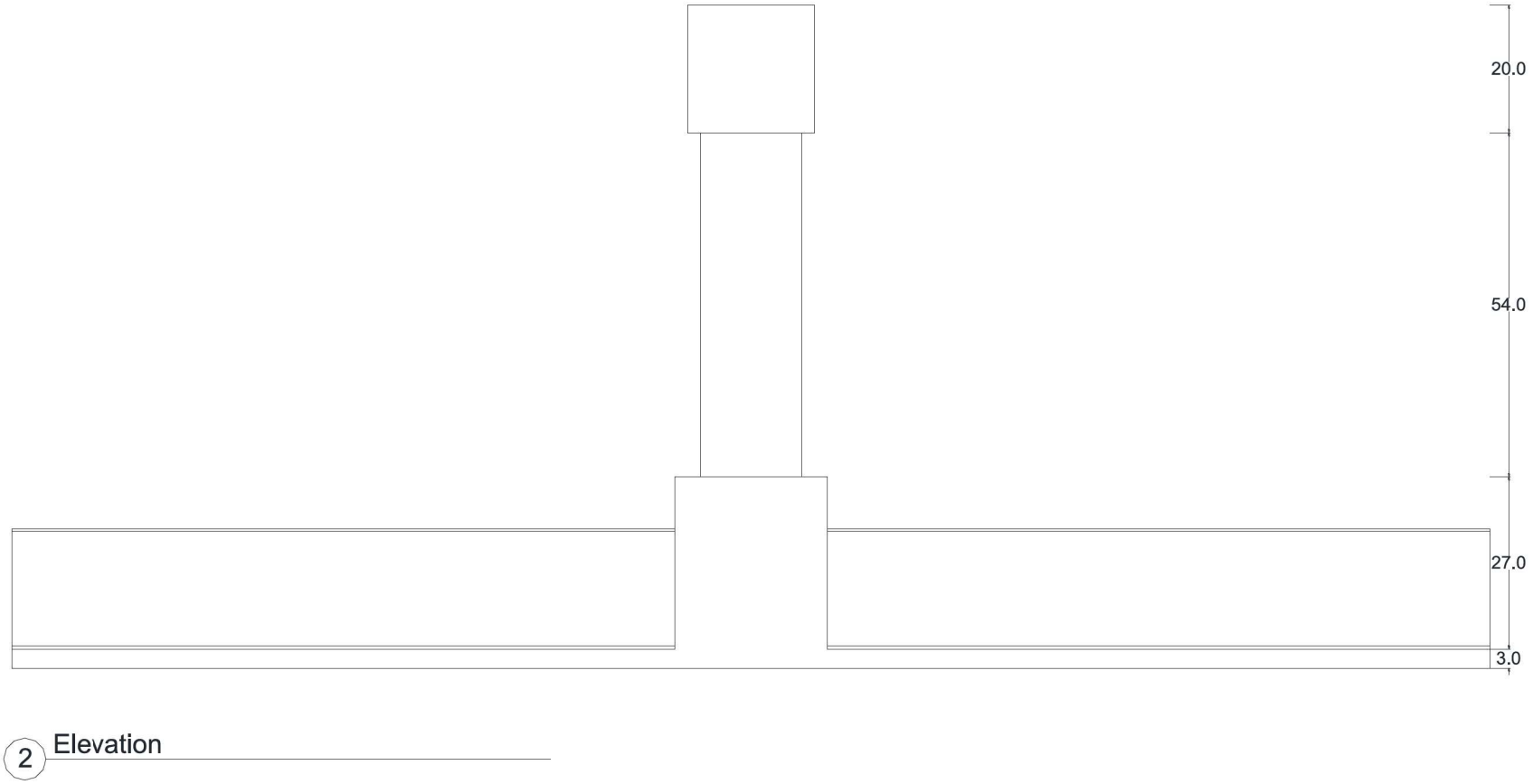


*Figure 3-3 Test specimen elevation.*

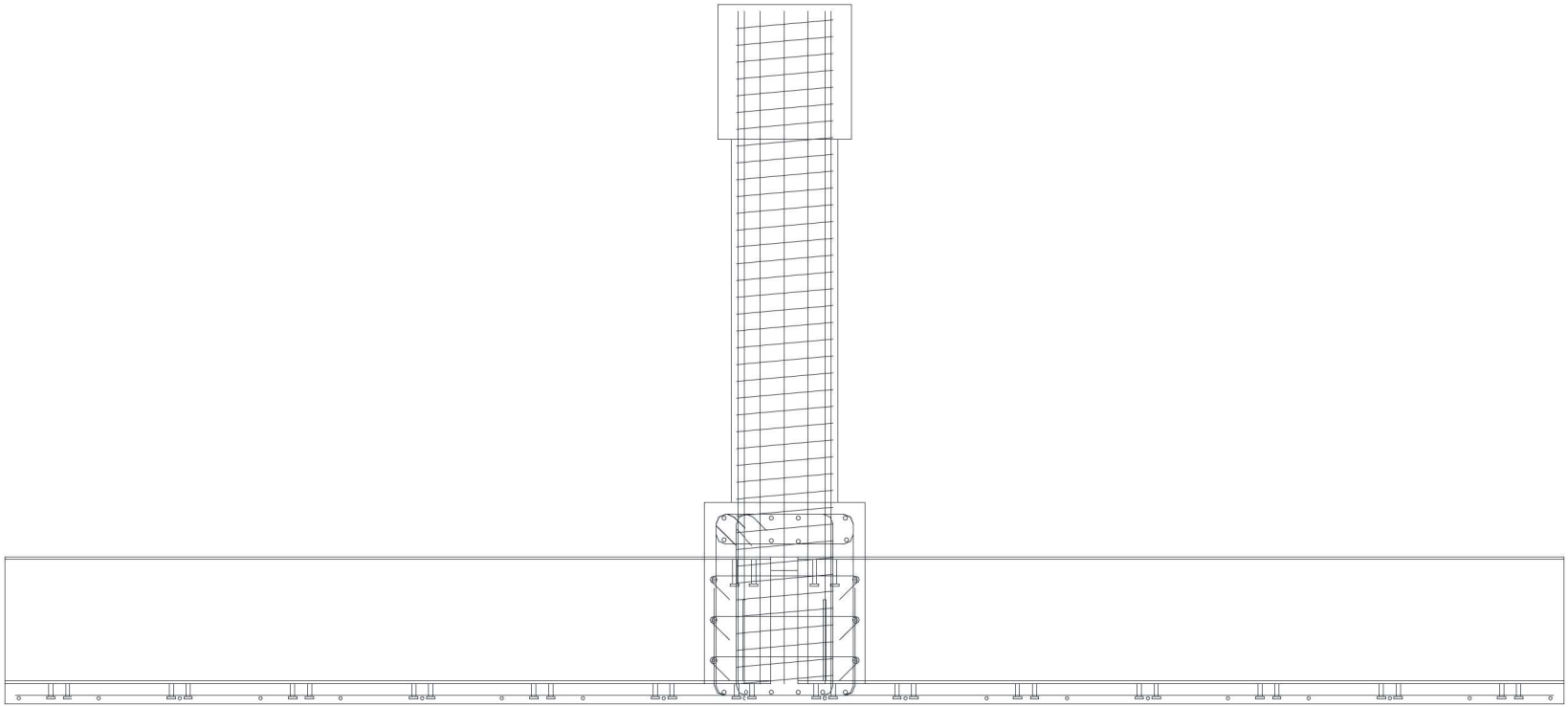


*Figure 3-4 Test specimen section.*

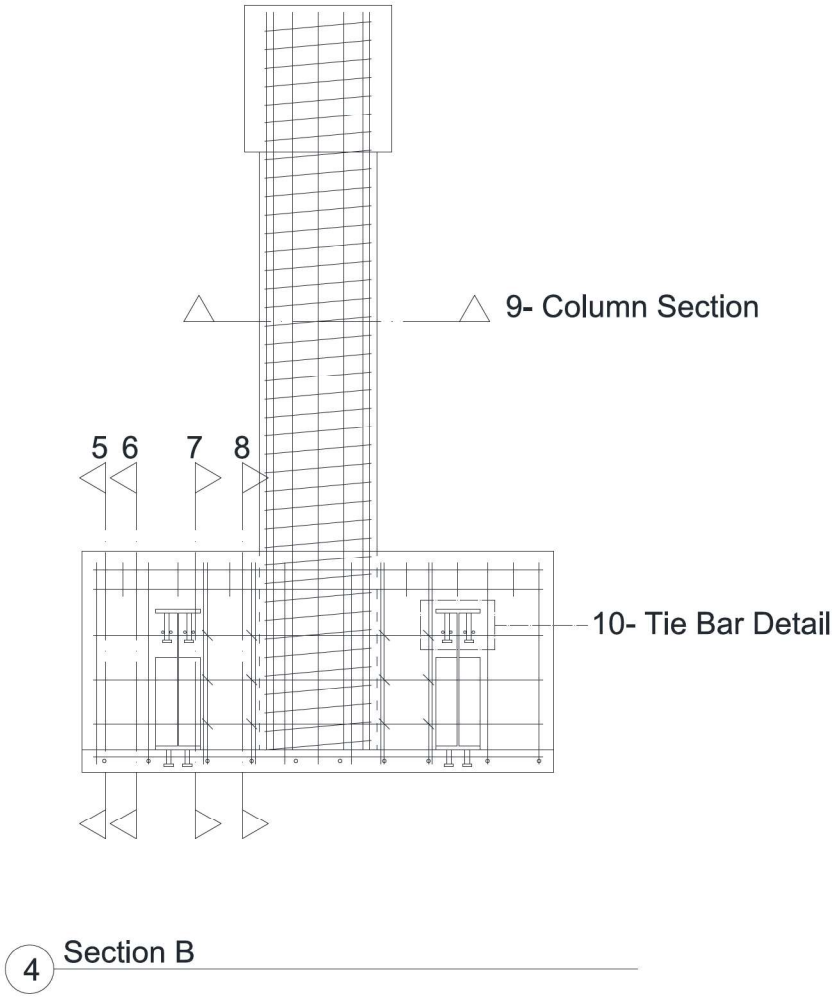


*Figure 3-5 Test specimen section.*

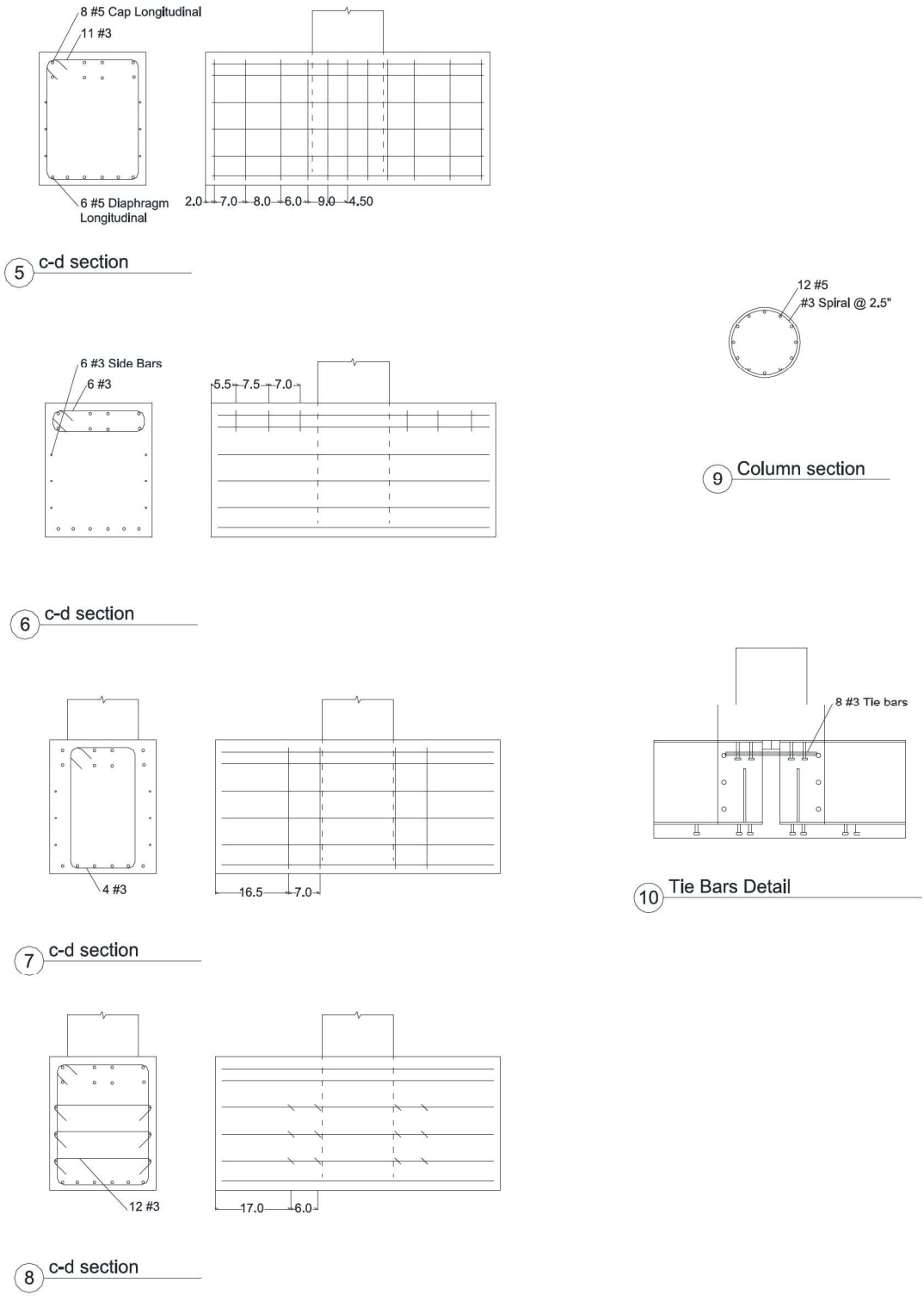


*Figure 3-6 Test specimen sections and details.*

## 3.1. Column

The column of the prototype bridge was designed by UNR research team. Based on the provided information, the diameter of the concrete column is 48 in. which is reinforced with 32#11 vertical bars and #7 hoop every 4 in. The compressive strength of concrete assumed to be 5000 ksi and the yield strength of reinforcement bars is equal to 60 ksi. The column was scaled down to 1/3 and redesigned for the component test. The diameter of the column is 16 in. which is reinforced with 12 #5 longitudinal bars and #3 spiral with 2.5 in. distance between hoops (Figure 3-7).

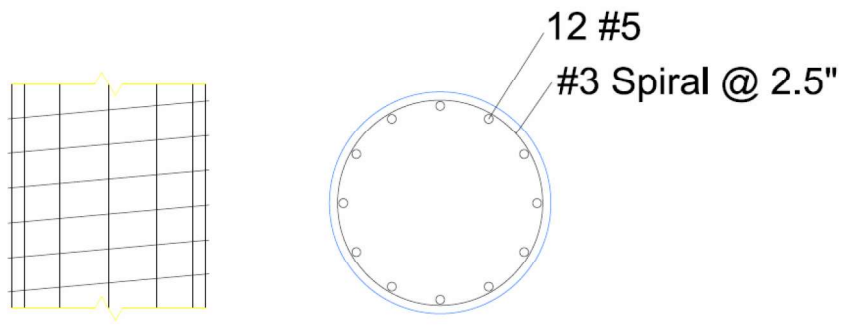


*Figure 3-7 Column section.*

The Section Designer program was used to observe the moment-curvature and calculating the column section properties. In the moment curvature plot, AASHTO/CALTRANS idealized bilinear curve represented by a dashed red line (Figure 3-8). The dotted green line represents over strength moment factor based on CALTRANS specification.

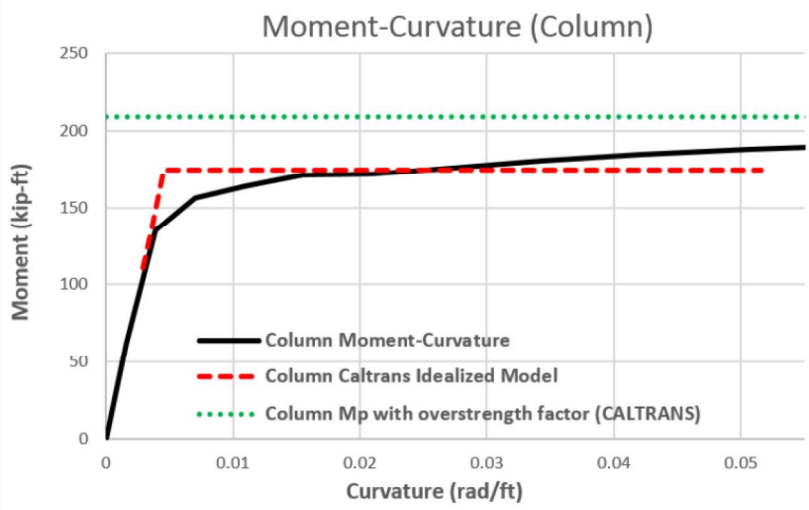


*Figure 3-8 Column moment-curvature for the one third scale*

## 3.2. Cap-beam and Diaphragm

Moment capacity of the column and cap beam in transverse direction (here cap beam refers to the concrete beam which comprises bent cap and concrete diaphragm) calculated by a Moment-

Curvature analysis. The finite element software ANSYS used to compute the moment capacity of the system in longitudinal direction (traffic direction). Notice for the moment curvature analysis in the transverse direction, the section is not symmetric, therefore analysis conducted for both negative and positive moments and the minimum considered for comparison with the column capacity.

According to CALTRANS, bent cap shall be designed as a capacity protected member and remained essentially elastic for flexural forces once the column reaches its over-strength moment capacity. The capacity design approach guarantee the super structure and bent cap have enough demand strength to carry transferred forces from the column at the ultimate load level. The expected nominal moment capacity $M_n$ of the capacity protected members can be computed using moment curvature analysis. The expected nominal moment capacity shall be based on expected material property when concrete strain reaches 0.003 or the steel strain reaches $\varepsilon^R_{su}$. Reduced ultimate tensile strain ($\varepsilon^R_{su}$) is equal to 0.09 for #10 bars and smaller, and is equal to 0.06 for #11 and larger. Following Figures show the moment capacity of the column and bent cap (longitudinal, Figure 3-9, and transverse direction, Figure 3-10) for the full scale and one third scale model. For the bent cap in longitudinal direction, the moment capacity of one girder calculated based on finite element model and two times of this capacity compared with moment capacity of the column.

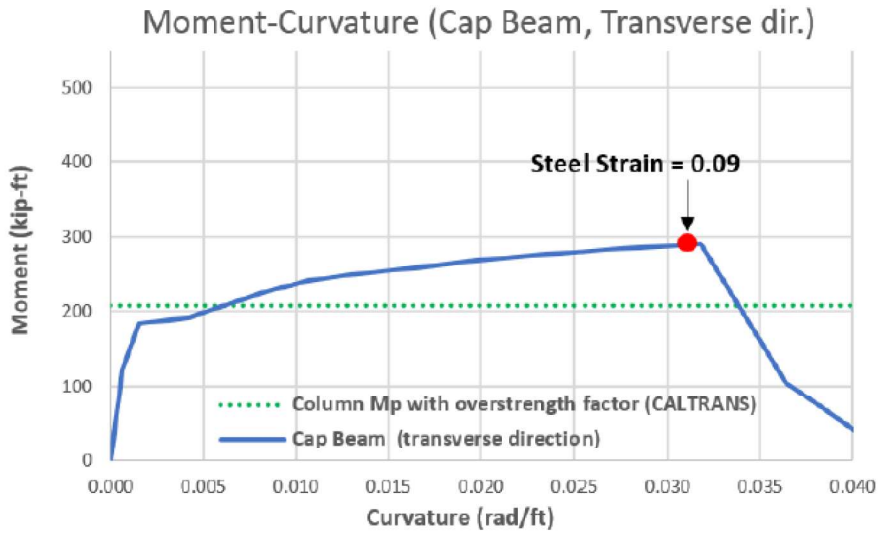


*Figure 3-9 Cap-beam moment-curvature in transverse direction.*

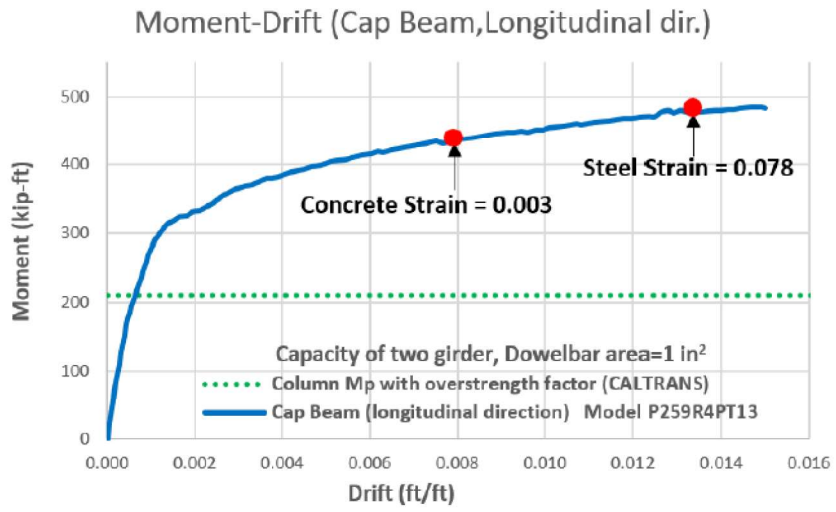


*Figure 3-10 Cap-beam moment-curvature in longitudinal direction.*

## 3.3. Girders and Deck

The prototype bridges consists of four W40x215 steel I-girders that support a 7 ½ in. deck. The deck is scaled down to 3 in and deck reinforcement was a mesh of #4 at 6 in. and the girders were scaled down to have the same stresses under scaled down demand forces (Figure 3-11 and Figure 3-12).

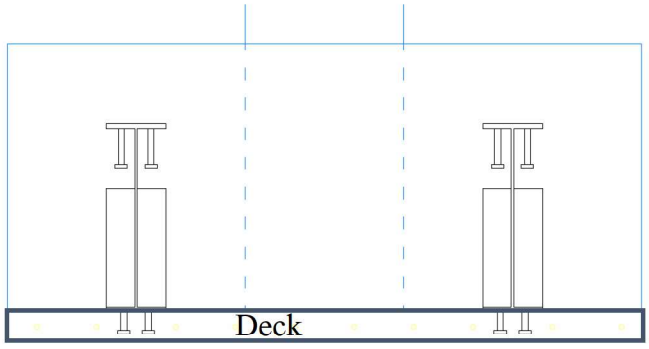


*Figure 3-11 Girders and deck view.*

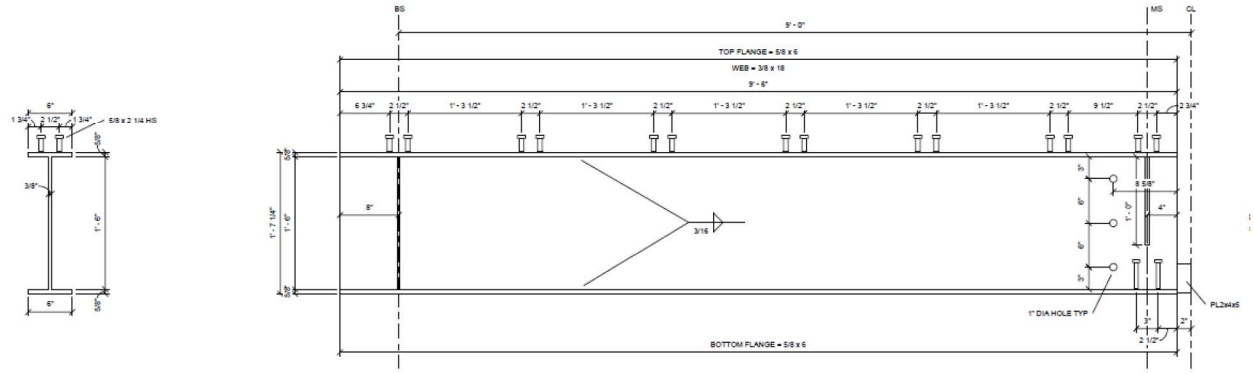


*Figure 3-12 Girder section and details.*

## 3.4. Connection Details

The SDCL connection detail suggested by the Phase I, numerical study, includes the following parts.

1. Steel blocks at the end of the compression flanges. These blocks are to pass the compression forces between the girders. The size of the steel blocks is 2"x2"x6" based on the size of the girders. The width of the block is equal to the width of the girder's flange and the height of it is suggested by the non-seismic design provisions of SDCL to be about 1/6 of the height of the girder. The blocks are welded to the end of the compression flanges.
2. Tie bars between the shear studs on the compression flange. These ties are to pass the maximum demand tension forces between girders.
3. End stiffeners. The stiffeners from the non-seismic version of the SDCL connection had to be modified to have space for passing the tie bars between the compression flanges. These stiffeners are to pass the compression from the top flange to the concrete and also grabbing the concrete under tension forces in the girder.
4. Additional deck reinforcement in the connection area. These reinforcement are to pass the tension forces between the top flanges of the girders. These additional deck reinforcement is incorporated in the deck design.

These details are to be capacity protected and remain essentially elastic during the force transfer. A schematic view of these details and the connection is shown in Figure 3-13. The constructed detail of the specimen in this area is shown in Figure 3-14

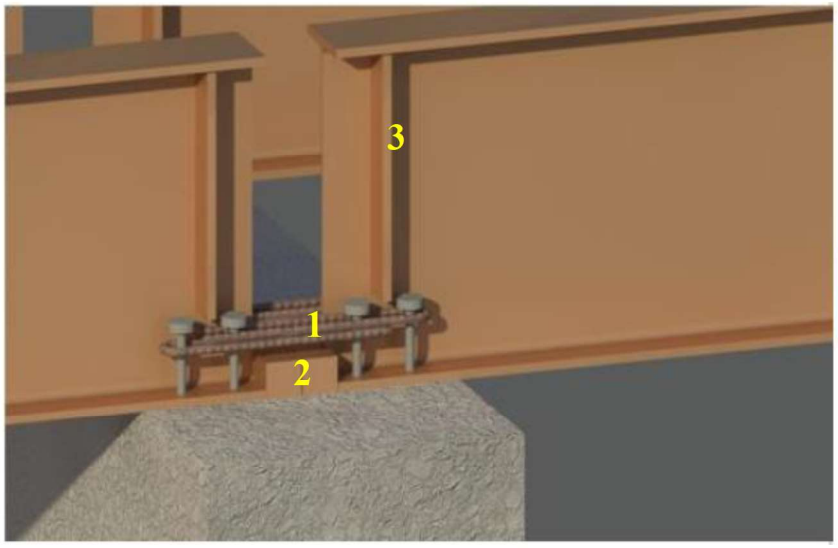


*Figure 3-13 Schematic view of connection details.*


*Figure 3-14 View of the connection detail as built.*

## 3.5. Test Setup

After investigating different test set ups for the component test, it was decided to construct a test set up similar to experimental testing conducted at the University of California - San Diego (Jill Patty, 2001). The main goal of this test is checking the detail which connects steel girders to each other inside the concrete diaphragm. When an integral bridge is subjected to longitudinal direction of earthquake loads, the deformation of column is double curvature with inflection point at the

middle of column length. The deflection and moment distribution along the girder and column is similar to Figure 3-15. The amount of moment at mid high of column and dead load inflection point is equal to 0.0 and 0.3M respectively as illustrated in Figure 3-16. Therefore, specimen is going to be constructed in an inverted orientation (Figure 3-17). The length of girders is equal to distance from column to dead load inflection point. The support at two ends of girders were constructed as roller (Figure 3-18). To avoid lateral movements of the specimen a roller was placed at each end of the deck (Figure 3-19).

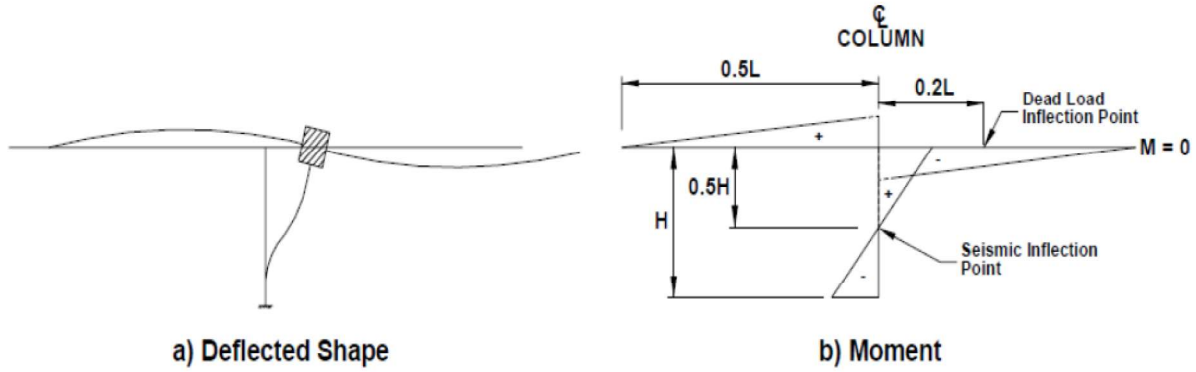


*Figure 3-15 Deflected shape and column moment diagram under longitudinal component of earthquake (Patty, 2001).*

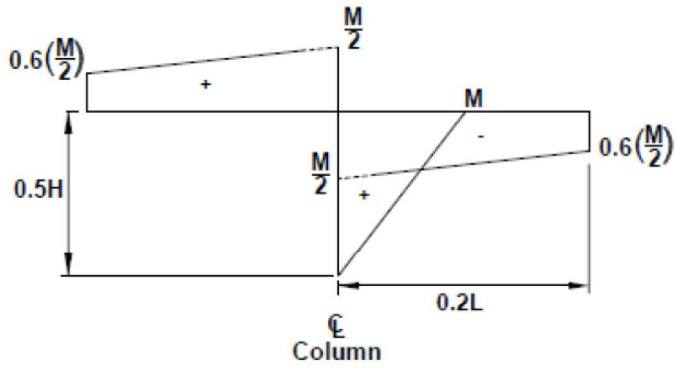


*Figure 3-16 Amount of moment at boundary condition of specimen (Patty,2001)*

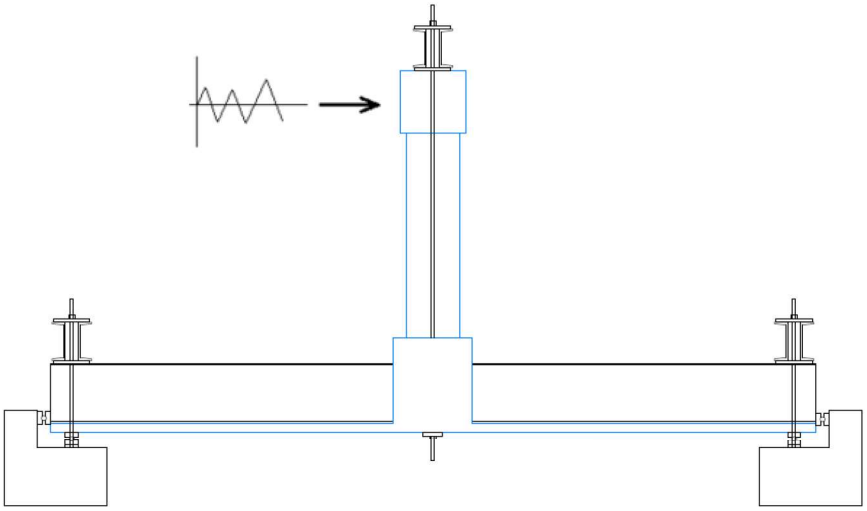

*Figure 3-17 Schematic view of test set up.*

*Figure 3-18 Roller support under the specimen.*

*Figure 3-19 Roller at the end of deck to control lateral movements.*

Based on the provided document by University of Nevada – Reno, a bridge with two span, each span equal to 100 feet was considered for the experimental test. The substructure of this bridge in the middle pier comprise two columns, and the superstructure include four steel girders and the reinforced concrete deck. The columns are connected monolithically to the bent cap. The design strategy for the component test is similar to a bridge with ductile substructure and an essentially elastic superstructure. Accordingly, the plastic hinges should form at end of the columns. Due to the symmetry behavior of the bridge, it was decided one column with two girders to be constructed in the structures lab. A schematic view of the component test shown in Figure 3-20. Figure 3-5 shows the test set up at Florida International University Structures Laboratory before testing.

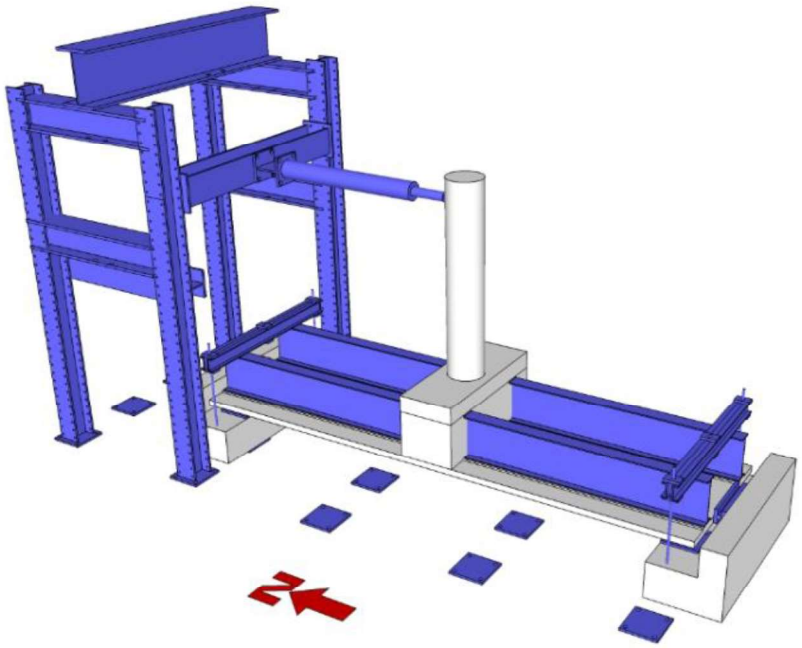

*Figure 3-20 Schematic view of the component test.*


*Figure 3-21 Component test set up before testing.*

## 3.6. Construction of the test specimen

Following the proposed inverted test setup, the construction of the specimen was a challenging task. It was decided to cast the specimen in three different steps.

1- Casting deck up to the girder flanges (3 in.)
2- Casting cap-beam and diaphragm up to the column (+27 in.)
3- Casting the column and loading cap (+74 in.)

These steps are shown in the Figure 3-22. Figure 3-23 to Figure 3-27 show the sequence of construction at different steps. Figure 3-28 shows the completed test specimen.

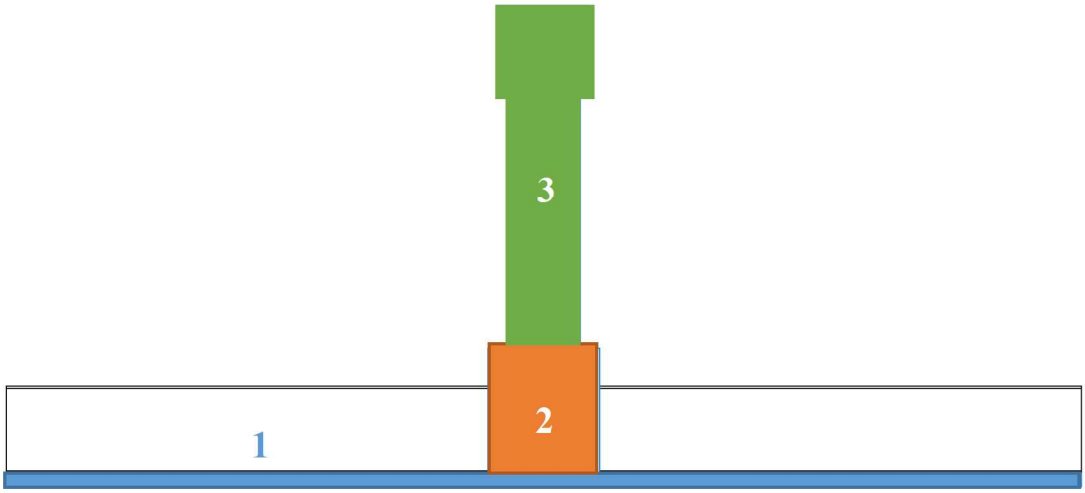


*Figure 3-22 Construction sequence for the test specimen.*

*Figure 3-23 Specimen before casting step 1.*

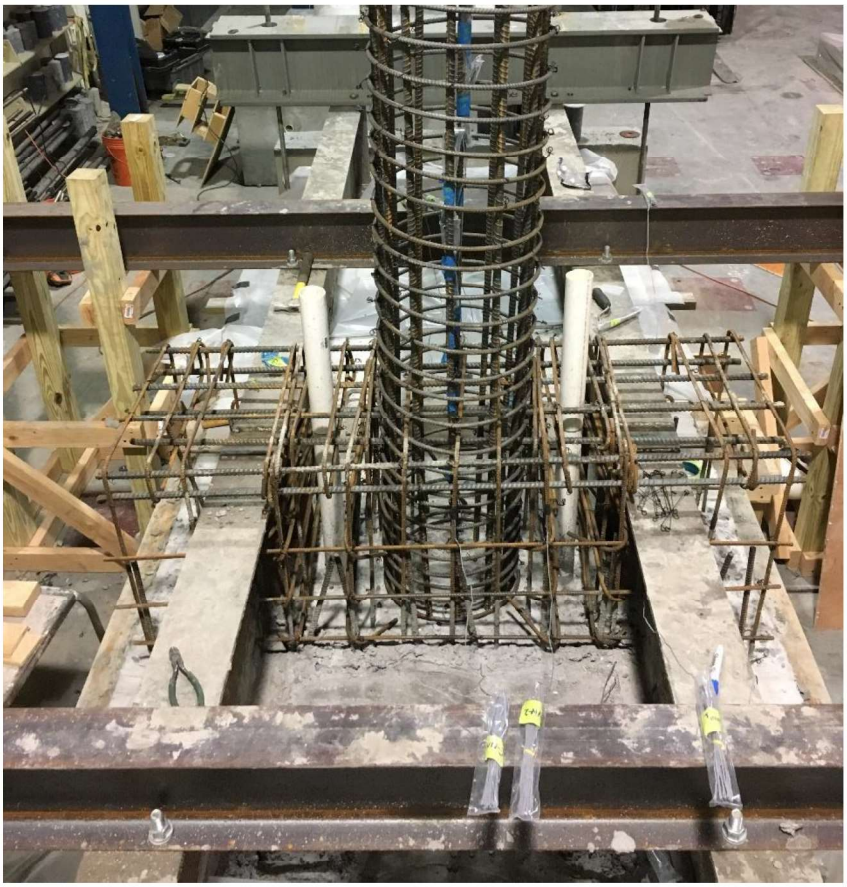

*Figure 3-24 Step 1 of the construction.*

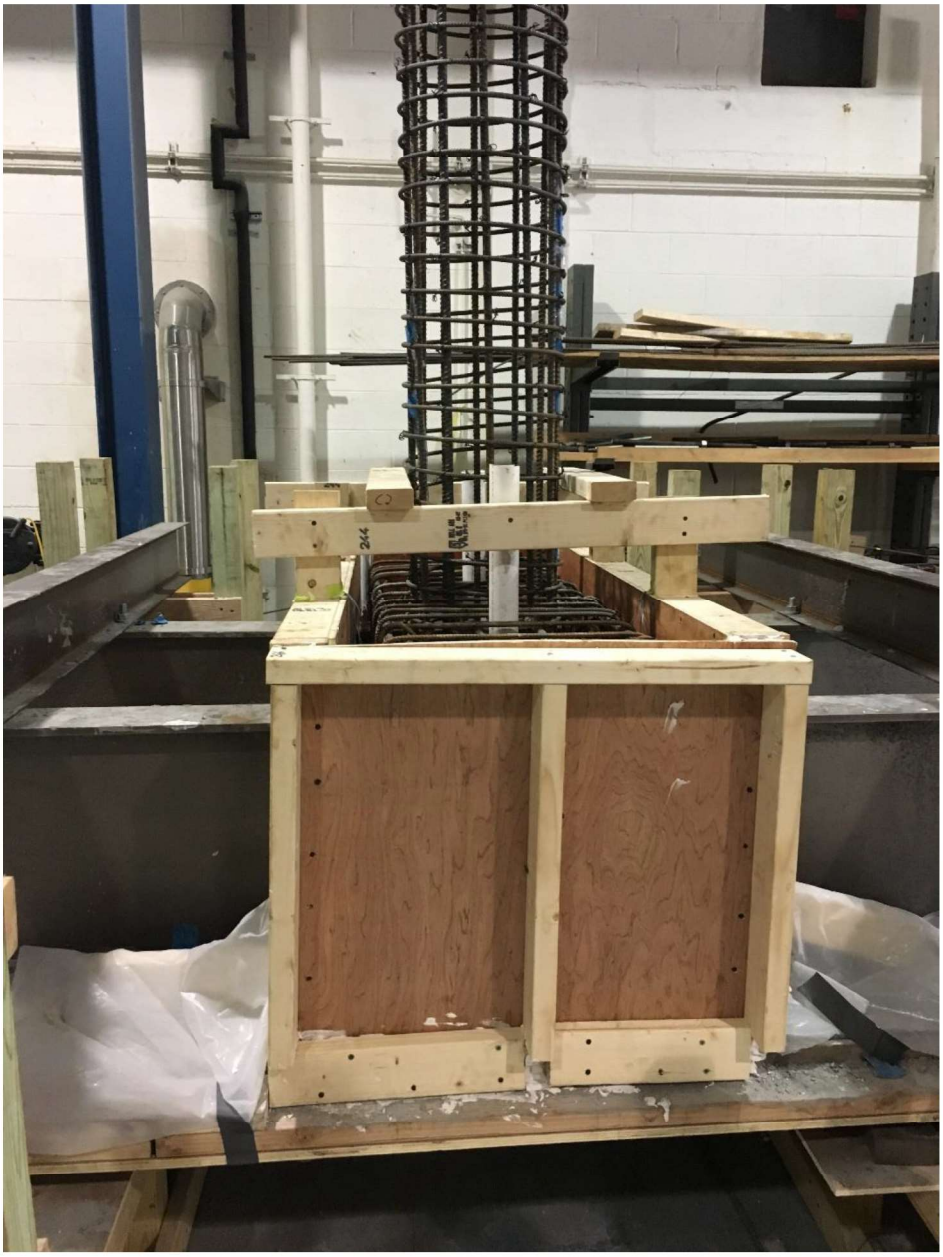

*Figure 3-25 Formworks for step 2 of construction.*

*Figure 3-26 Step 2 of construction.*

*Figure 3-27 Step 3 of the construction.*


*Figure 3-28 Test specimen after construction and removing formworks.*

## 3.7. Loading setup and protocol

Axial loads were applied with two 70-kip hollow core jacks on a spreader beam on top of the column cap. Lateral loads were applied by 140-kip hydraulic jack supported on a steel frame (Figure 3-30).

The specimen was loaded axially to 10% of the nominal axial capacity of column at the beginning of the test. Lateral load was applied to specimen from north to south (push) up to near twice the expected yield displacement of the column. From the captured results and the slops of the curve, before and after yielding, the yield displacement of the column ($\Delta_y$) was calculated. From this point the loading direction was reversed and the specimen was loaded to $-\Delta_y$ and after that two cycles with same displacement level ($1\Delta_y$) were applied to the specimen. Then the slow cyclic loads were applied to the specimen based on the calculated yield displacement ($\Delta_y$) with increments of $1\Delta_y$ and 3 cycles at each displacement level up to the failure of the specimen.

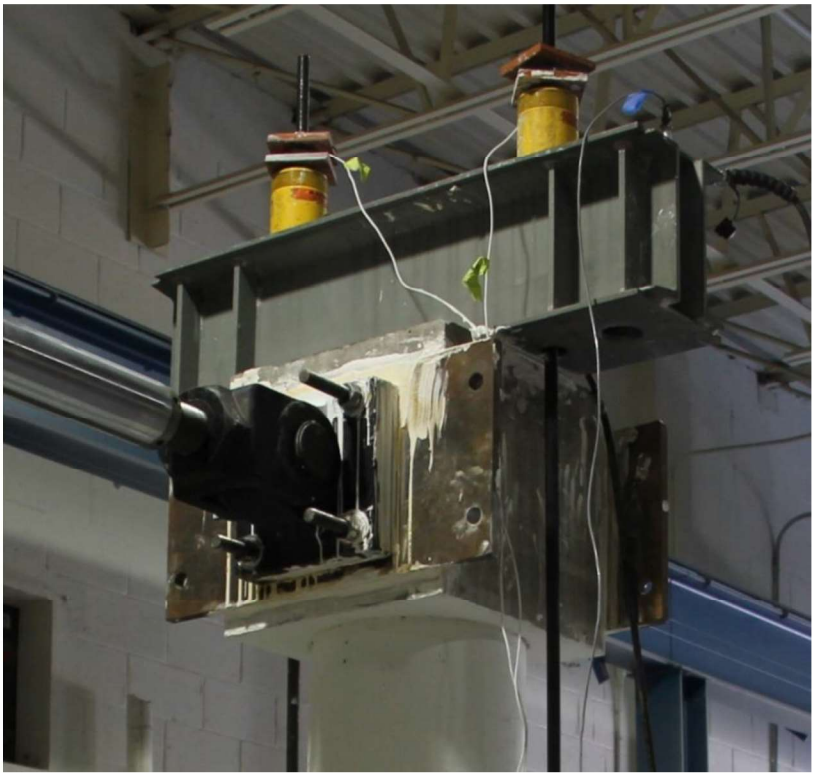

*Figure 3-29 Hydraulic jacks for applying axial load.*

*Figure 3-30 Hydraulic jack for applying lateral load.*

## 3.8. Instrumentations

### 3.8.1. Load and Displacement

Measuring the loads was done by using both load cells and pressure transducers. Lateral load was measured by eight 50000-lb donut load cells, 4 for pushing and 4 for pulling, on the connection of hydraulic jack and the support frame, Figure 3-31. The pressure transducers were measuring the oil pressure at both ends of the hydraulic jack (pressure at the back $P_b$ acting on the area $A_b$ and pressure at the front $P_f$ acting on the area $A_f$), and the lateral load was calculated with the equation (3-1).

$$F_l = A_b P_b - A_f P_f \qquad (3\text{-}1)$$

Axial load was measured by two 50000-lb donut load cells, one on each rod. A pressure transducer was also measuring the pressure on the hydraulic cylinders to check the axial load.

The displacement were metered by string potentiometers from both sides of the specimen to have a reliable measurement, Figure 3-32. To consider for the probable movements of the specimen during the lateral loadings, two linear potentiometers (LVDT) were used at one end of the specimen to measure the change in the distance between the specimen and support.

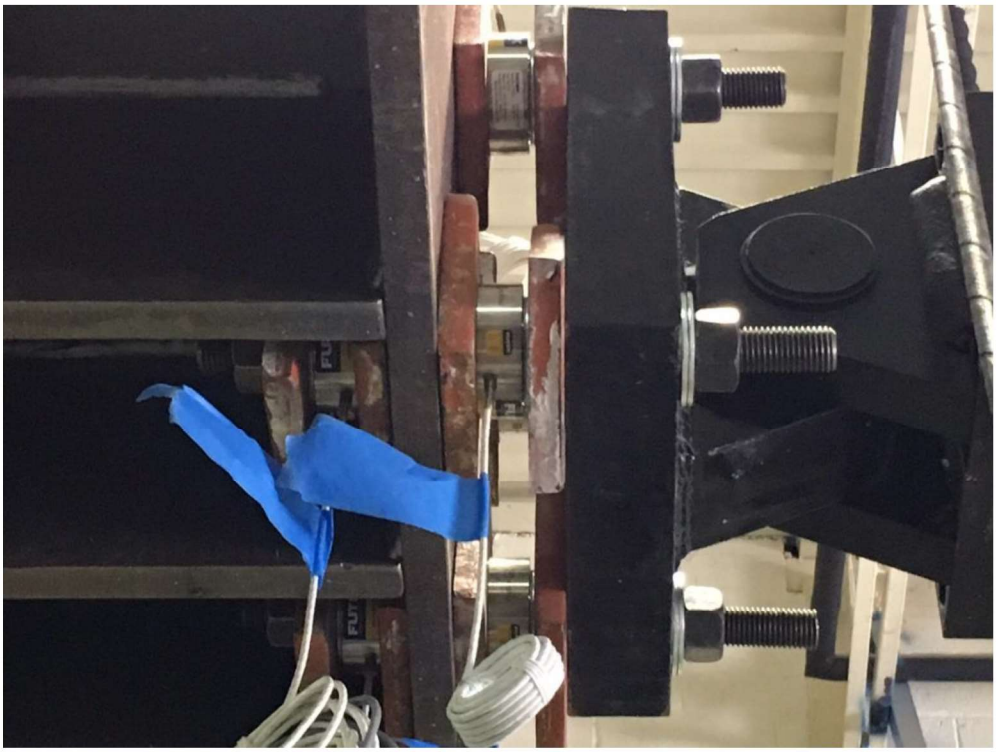

*Figure 3-31 load cells for measuring the lateral load.*

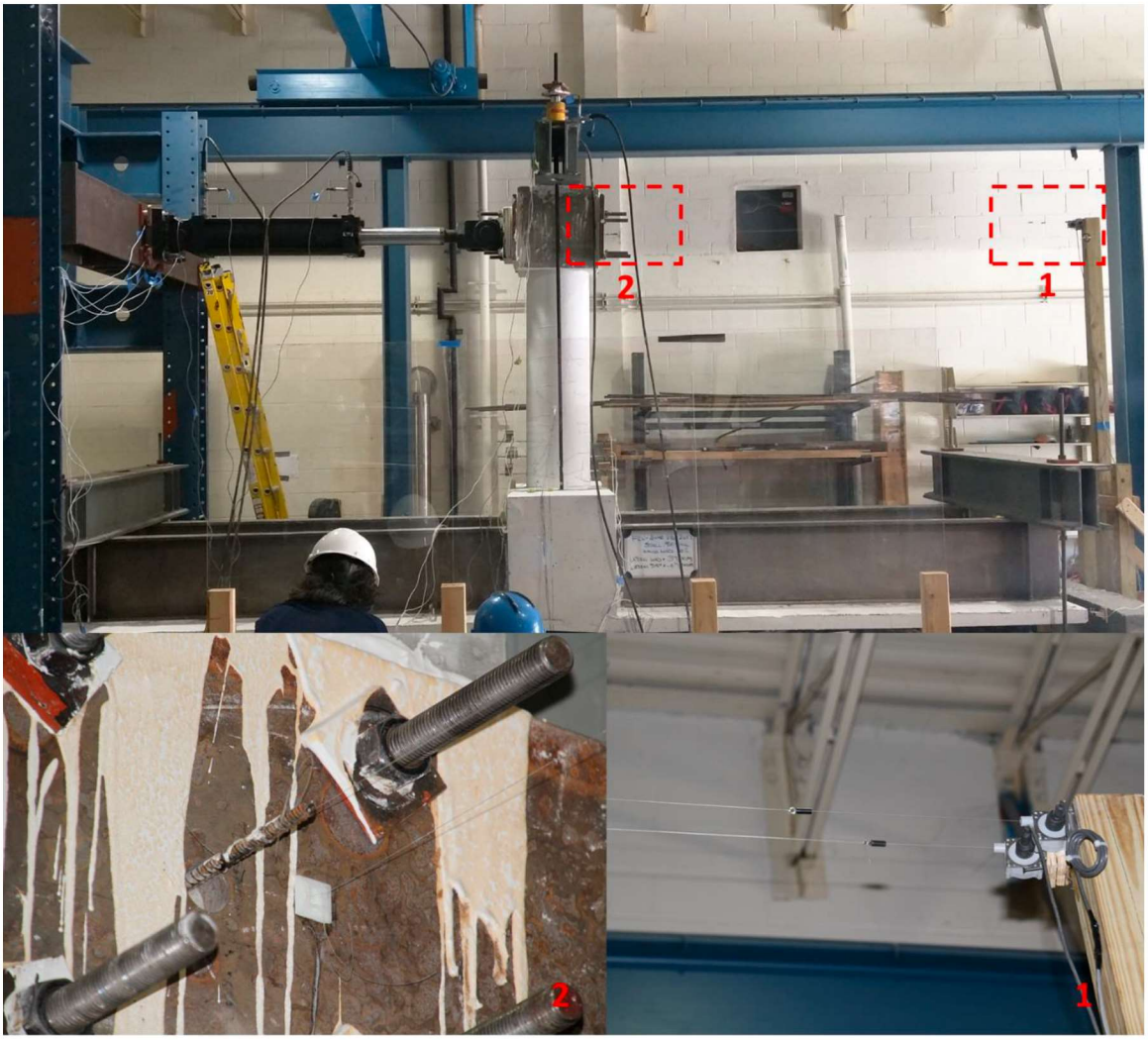


*Figure 3-32 Displacement measuring.*

### 3.8.2. Curvatures and Rotations

Rotations of the column section were measured at 3 levels by two linear potentiometers (LVDT) on each level at both sides, Figure 3-33. The rotations of each level were measured with respect to the bottom level, and the lower level to the cap-beam surface. The curvature of the level is calculated from the differential rotation divided by distance between levels.

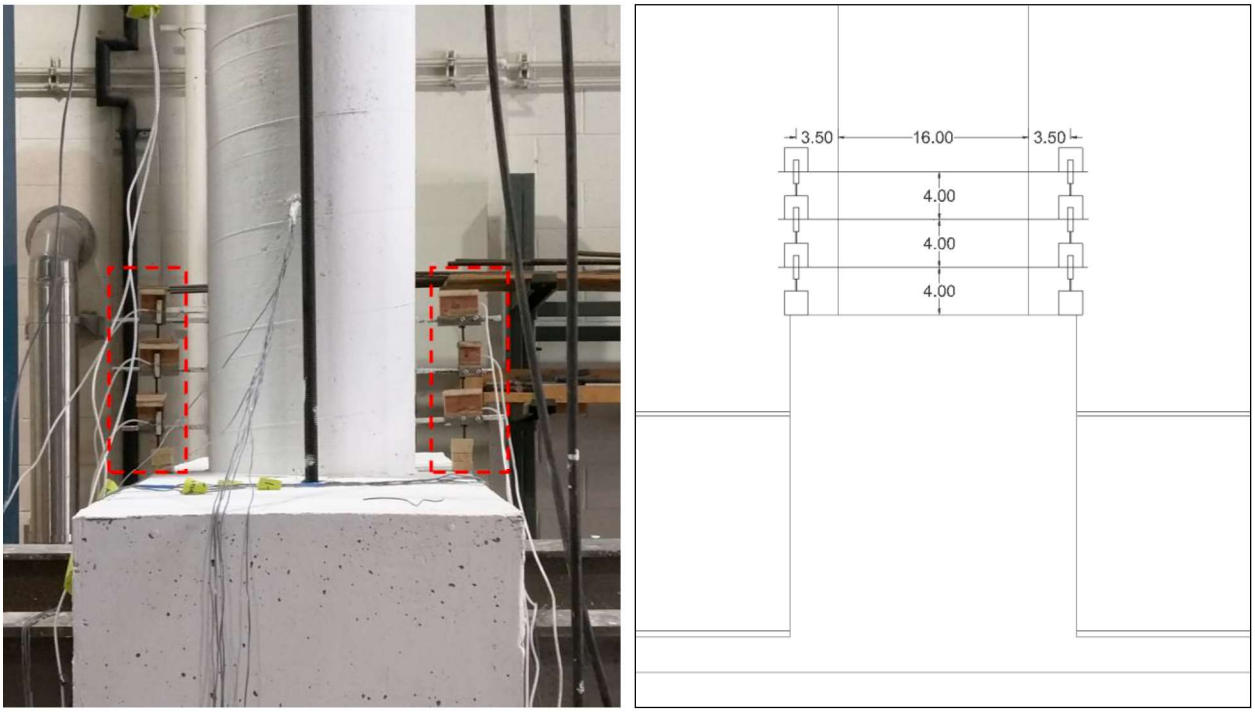


*Figure 3-33 Rotation and Curvature measurement on the column*

### 3.8.3. Strains

During the test, total of 27 post-yield strain gauges were used to measure strains on the reinforcing steel bars and the girders. 7 strain-gauges were placed on the column longitudinal reinforcements, 3 on the north side and 4 on the south side, with different distances from the cap-beam face. Details for these gauges are depicted in Figure 3-34. 7 strain-gauges were measuring the strains on the dowel bars at the position of assumed diaphragm and cap-beam connection. These strain-gauges are shown in Figure 3-35. 2 strain-gauges were attached to the tie bars between the compression flanges on the west girders, shown in Figure 3-36. Strain measurement on the deck longitudinal reinforcement were done by 9 gauges outside the diaphragm, 4 on south and 5 on north side of the deck, shown in Figure 3-37. 2 strain-gauges were installed on one of the girders, on bottom and top flange 12 inches from the diaphragm.

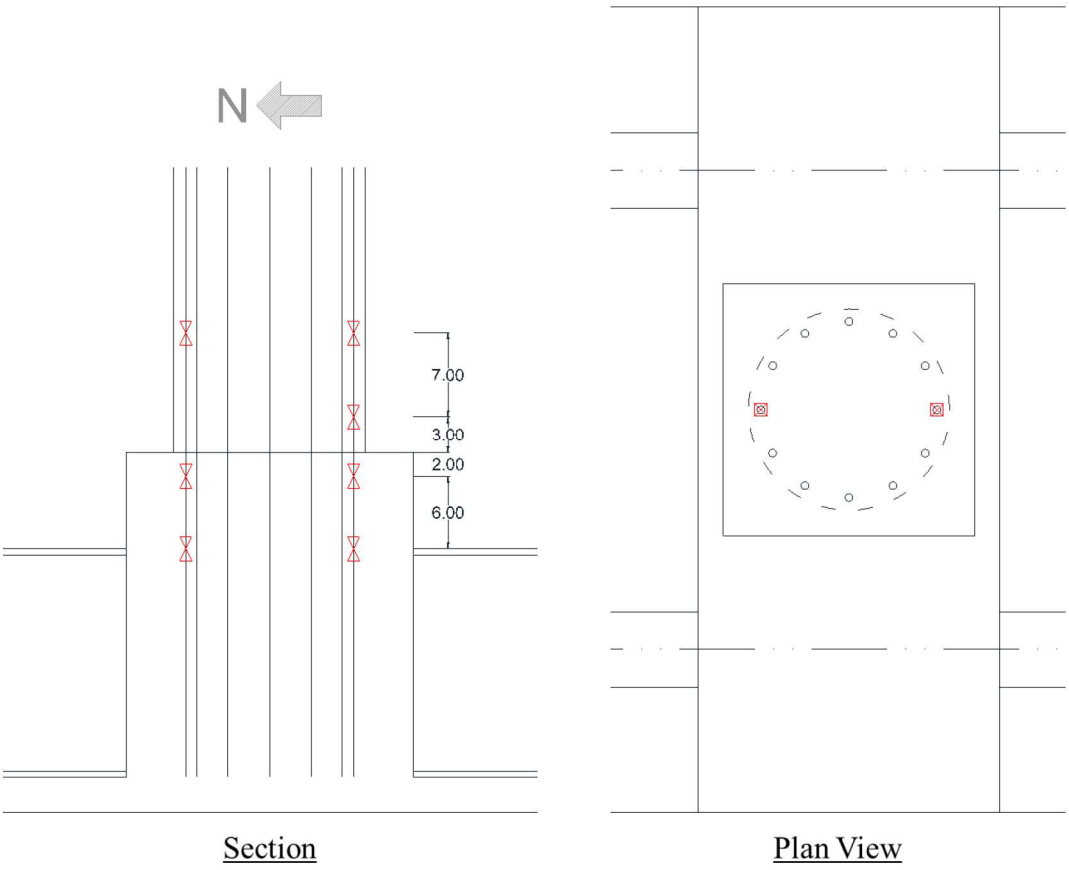


*Figure 3-34 Strain-gauges on the column.*

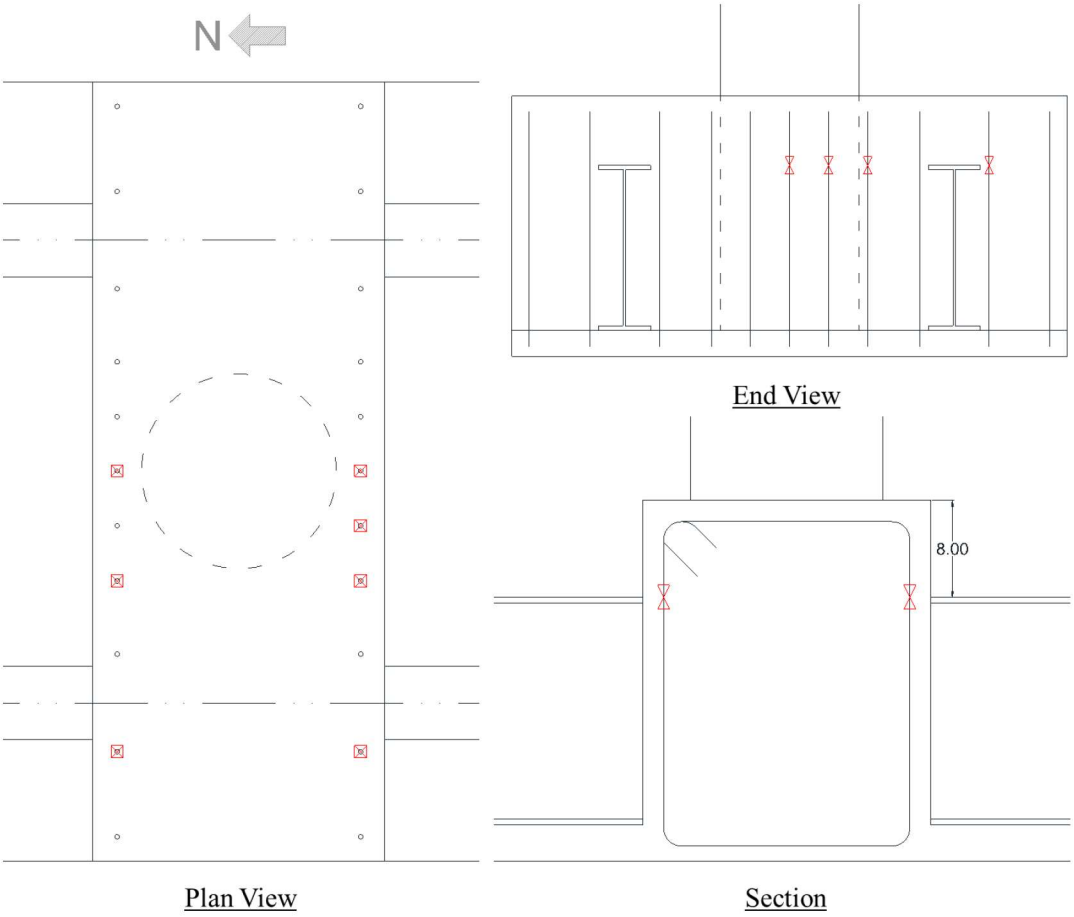


*Figure 3-35 Strain-gauges in the cap-beam-diaphragm.*

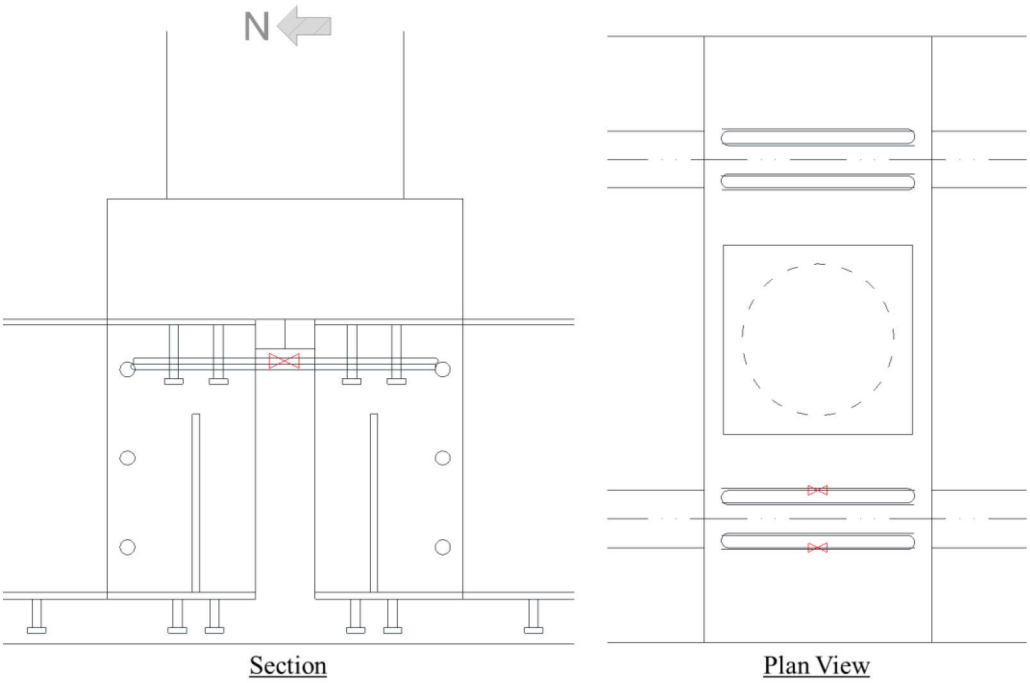


*Figure 3-36 Strain gauges on tie bars.*

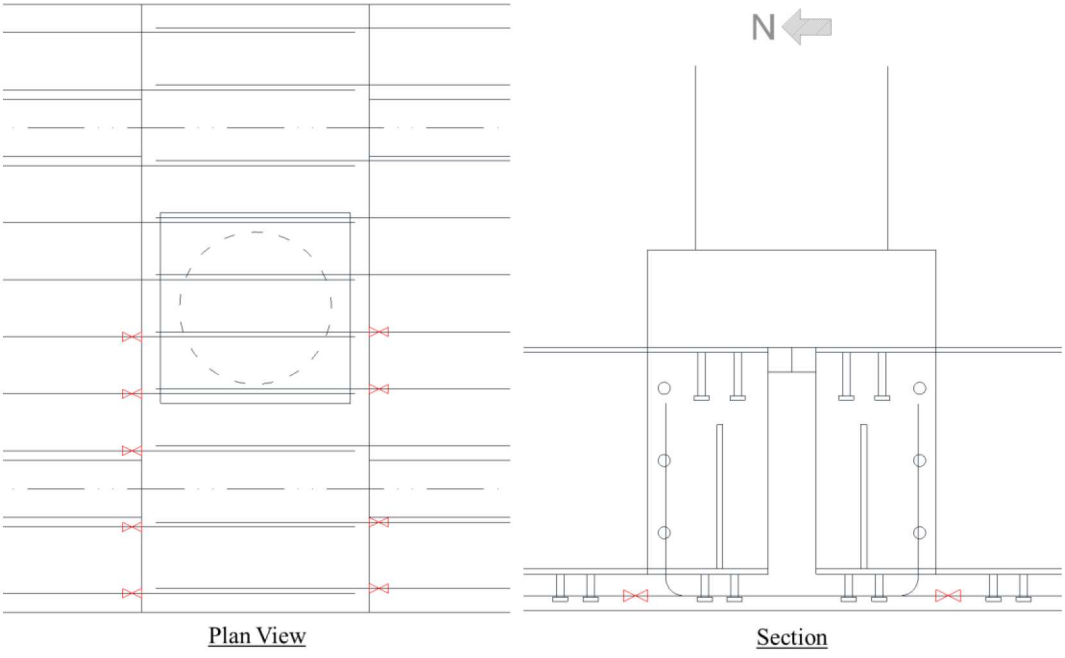


*Figure 3-37 strain gauges on deck reinforcements.*

# 4. Component Test Results

## 4.1. Material Testing

### 4.1.1. Concrete

The measured strength of concrete samples from different steps of construction are shown in Table 4-1. 4-inch diameter and 8-inch height plastic cylinders were used to sample concrete, Figure 4-1 shows the concrete samples on the day of test. The concrete material testing was done at 28 days after casting of each step and a day after the test. Three samples were used for tests but only the average values are reported.


*Figure 4-1 Sample concrete cylinders.*

*Table 4-1 Concrete cylinder test results*

| Construction step | Strength of concrete sample (psi) | |
|---|---|---|
| | 28 days | A day after test |
| Deck | 7287 | 8504 |
| Cap-beam, Diaphragm | 7249 | 8104 |
| Column | 4733 | 5224 |

### 4.1.2. Reinforcing steel

The reinforcing steel used were Grade 60 ASTM A706 bars in three sizes of #3, #4 and #5. The mechanical properties of the tested samples of the bars are shown in Table 4-2.

*Table 4-2 mechanical properties of reinforcing steel*

| Bar size | Yield stress (psi) | Ultimate stress (psi) |
|---|---|---|

| | | |
|---|---|---|
| #3 | 74000 | 102500 |
| #4 | | |
| #5 | | |

## 4.2. Observations

The specimen was loading in South-North direction, loading from North to South was called Push and South to North was called Pull. The observed damages at the end of each third cycle with different displacements are shown in Figure 4-2. The first cracks was seen during the first cycle in push on the north side of the column in the first 12 in. from the cap-beam, Figure 4-3. First signs of crushing in the concrete also was seen during the first cycle, as the first cycle (Push) was loading to higher displacements than the theoretical yield displacement of the column, Figure 4-4. There was a significant drop (30%) in the maximum lateral load in the second and third cycle of loading (maximum displacement of $1\Delta_y$) comparing the first cycle. First yield in the reinforcement also occurred in the first cycle.

On the second cycle of $3\Delta_y$, the first crack was seen on the cap-beam. This crack was in the middle of the cap between two girders on the south side of the column, Figure 4-5. On $4\Delta_y$ displacement, cracks on the cap-beam were propagating, Figure 4-6. At the last cycle of $5\Delta_y$ the cap beam cover on the south side of the column started to spall, Figure 4-7 and Figure 4-8, at this stage the north side of the specimen just had minor cracks, Figure 4-9. By the end of the test most of the cap-beam cover on the south side of the column was cracked and was removed, Figure 4-10.

First buckling in the longitudinal reinforcement of the column happened during the pushing of third cycle of $6\Delta_y$ on the south most rebar of the column, Figure 4-11, and on the pulling side of same cycle the north most rebar was buckled. The test was ended after seeing the first fracture in the south side of the column during the pull in first cycle of $7\Delta_y$, Figure 4-12. The maximum axial load during the test was 112 kips (18kips increase). The specimen experienced 3 successful cycles of $6\Delta_y$ equal to 6.5% drift. During the test, the diaphragm and the deck remained intact without any cracks and yielding. Figure 4-13 shows the deck from the bottom after the test.

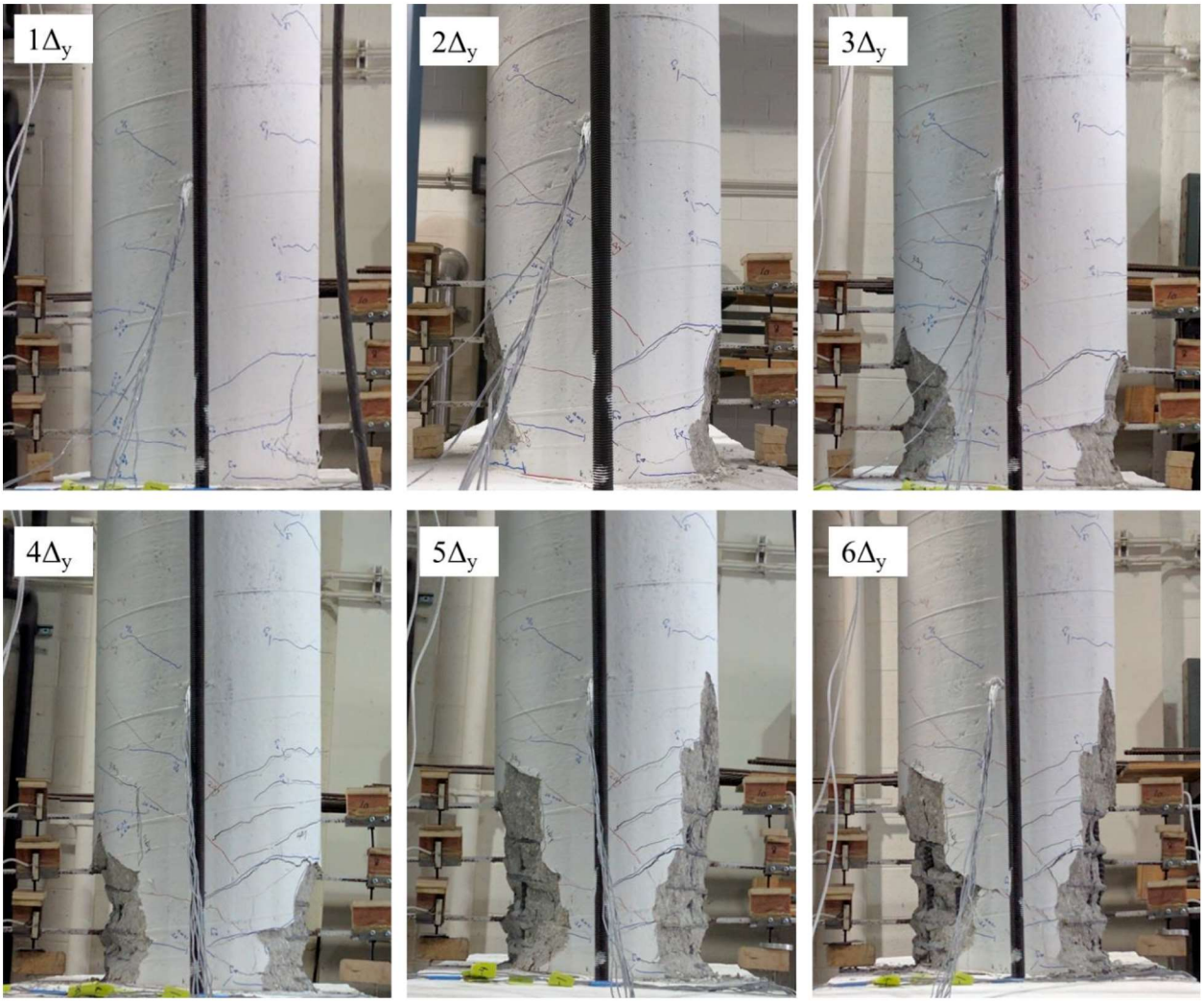


*Figure 4-2 View of the column at the end of each third cycle.*

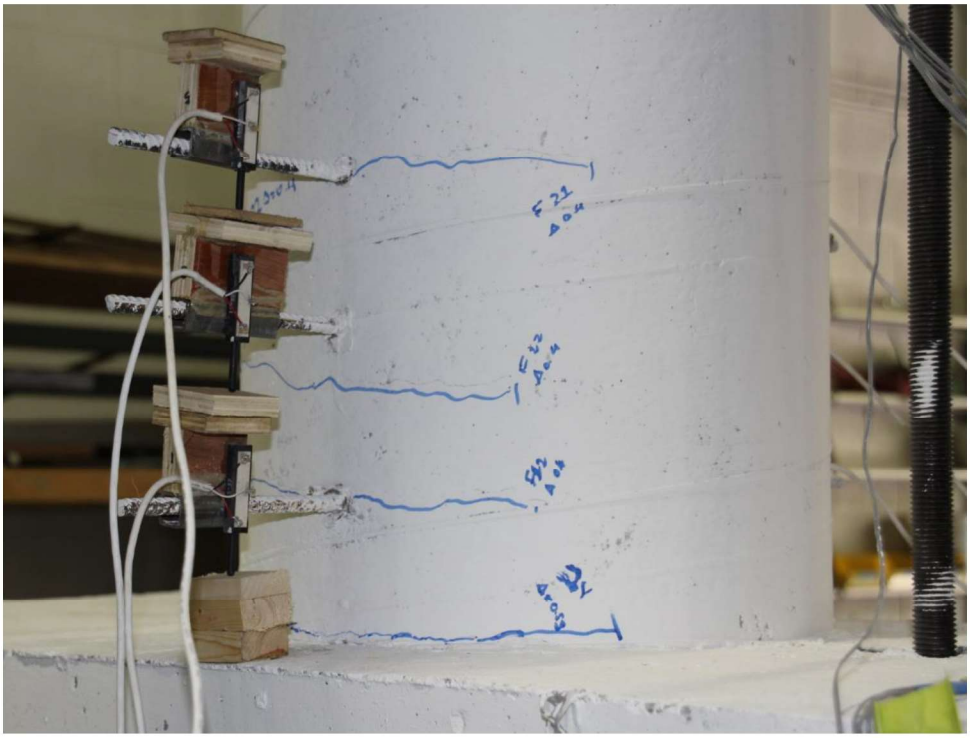

*Figure 4-3 Forming of first cracks in the North side of the column*

*Figure 4-4 Crushing of concrete on the North side of the column at $1\Delta_y$.*

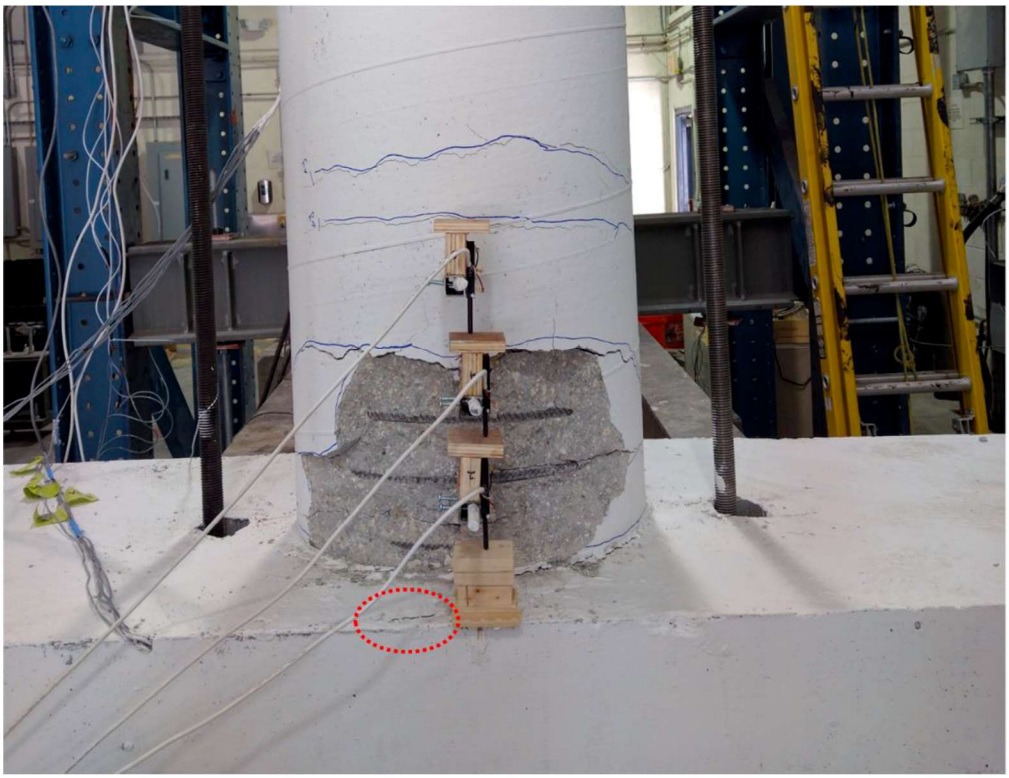

*Figure 4-5 First crack on the cap-beam at $3\Delta_y$.*

*Figure 4-6 Cracks on cap-beam at $4\Delta_y$ (south).*

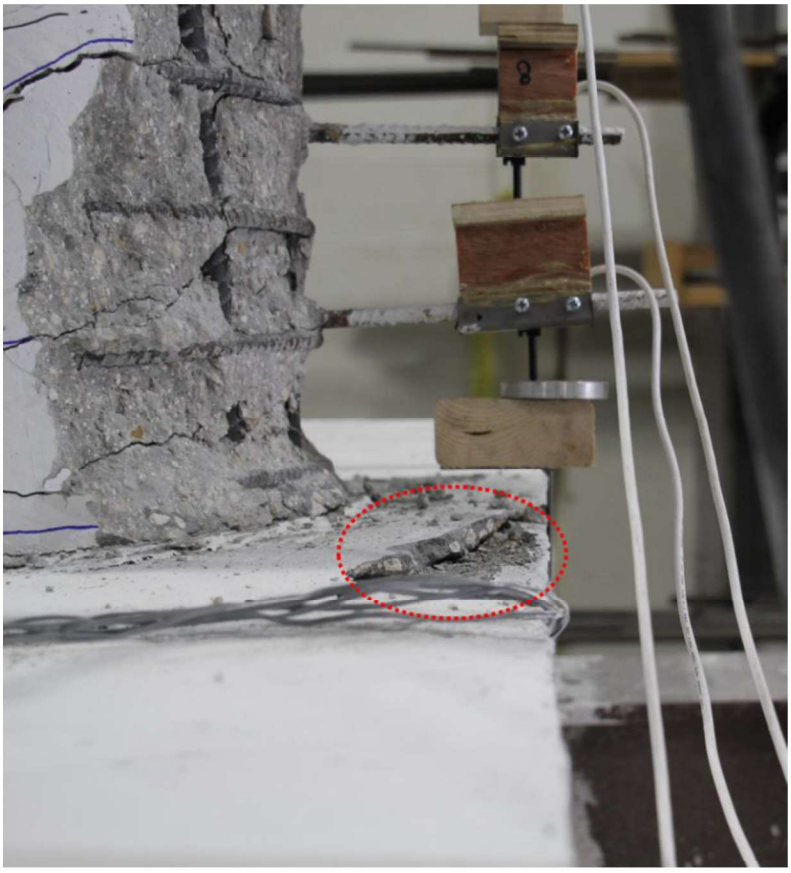

*Figure 4-7 Cap-beam cover spalling at $5\Delta_y$ (south of the column).*

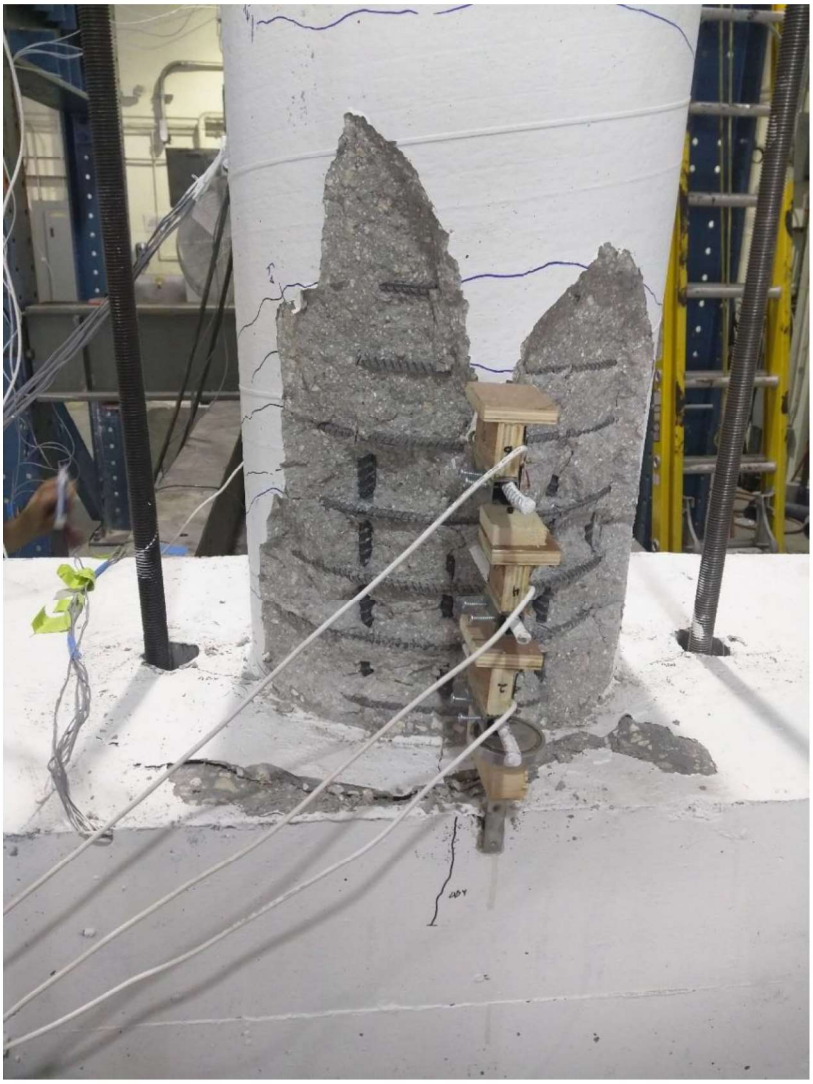

*Figure 4-8 Cap-beam cover spalling at $5\Delta_y$ (south of the column).*

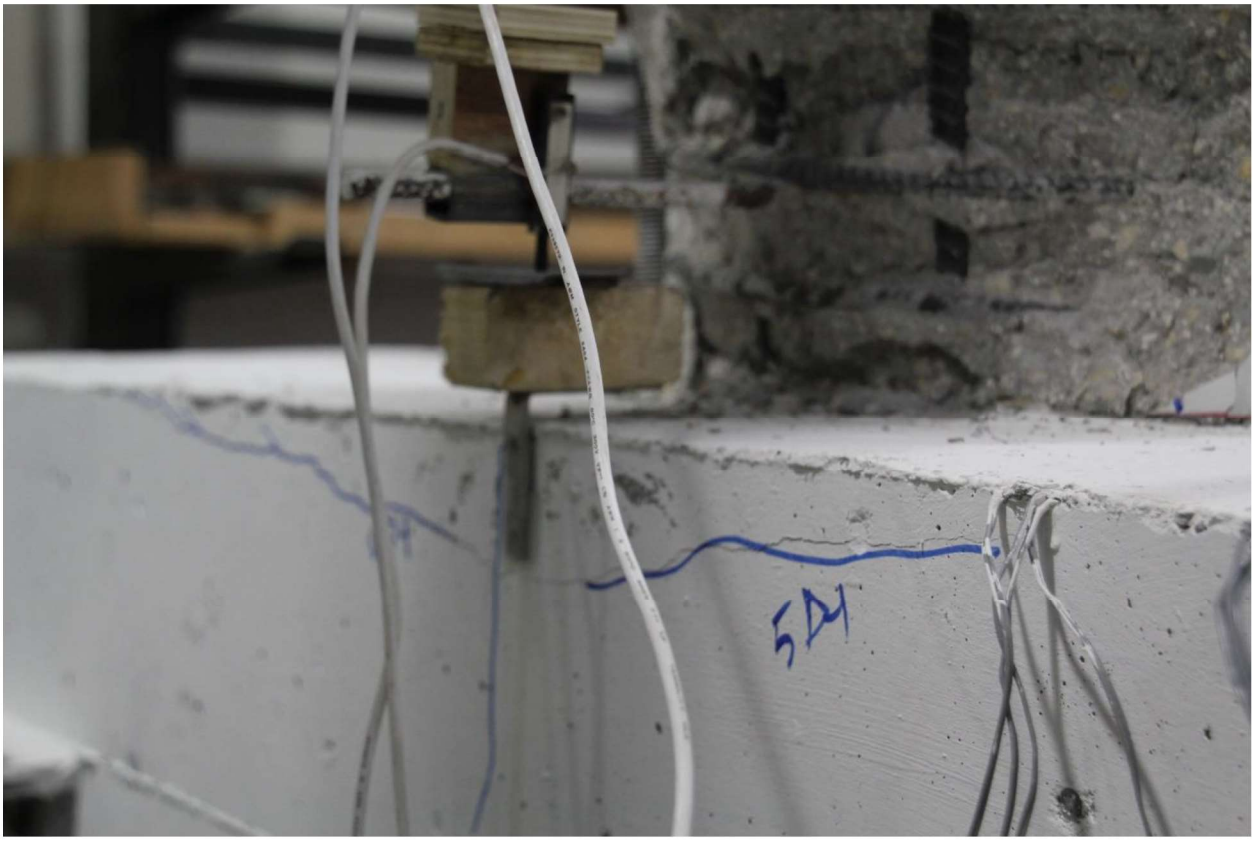


*Figure 4-9 Cracks on the cap beam at $5\Delta_y$ (north of the column).*

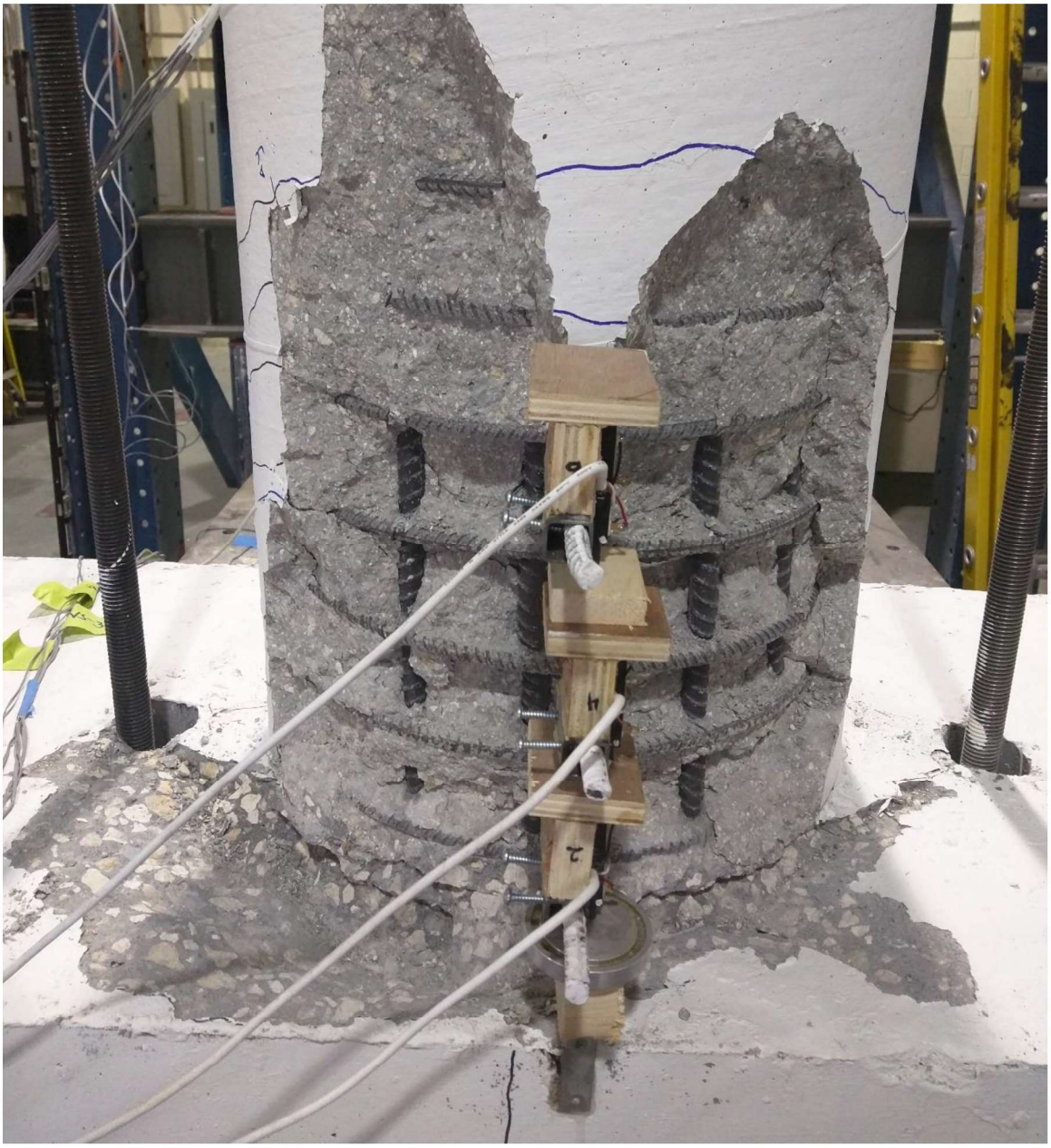

*Figure 4-10 removing cracked concrete of cap-beam cover (south) at the end of test.*

*Figure 4-11 First buckling in column longitudinal bars at $6\Delta_y$ (south).*

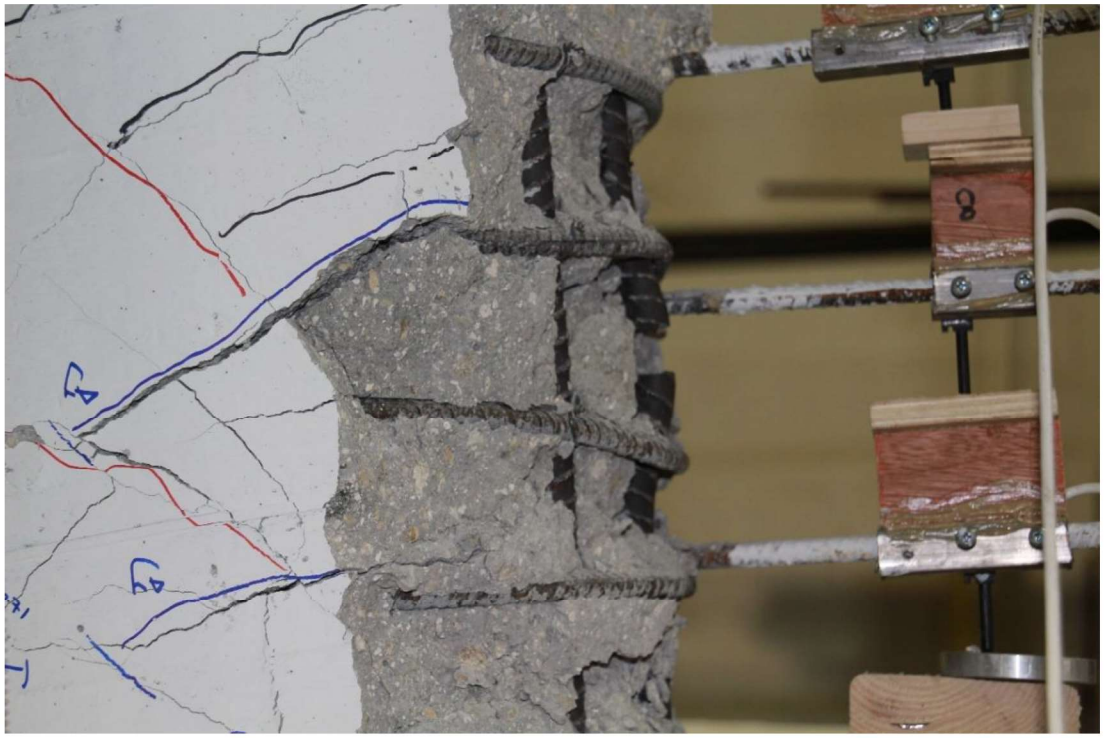

*Figure 4-12 Fracture in the column longitudinal bar at first cycle of $7\Delta_y$ (south).*

*Figure 4-13 Bottom of the deck at the end of the test.*

## 4.3. Force-Displacement Relationship

The load-displacement curves, Figure 4-14, are generated from data collected during two sessions of testing. The results from moment curvature analysis of column superposed with elastic superstructure (cap-beam, diaphragm, girders and deck), plotted on the same figure, shows a very good agreement between the experiment and analysis. This agreement was expected due to the conventional cast-in-place construction of the column. The specimen exhibited no strength degradation during the test before rebar fracture. The specimen was slightly stronger on the pulling side (south to north). The overall behavior of the specimen was symmetrical except for the first 3 cycle, where the loading was not symmetrical.

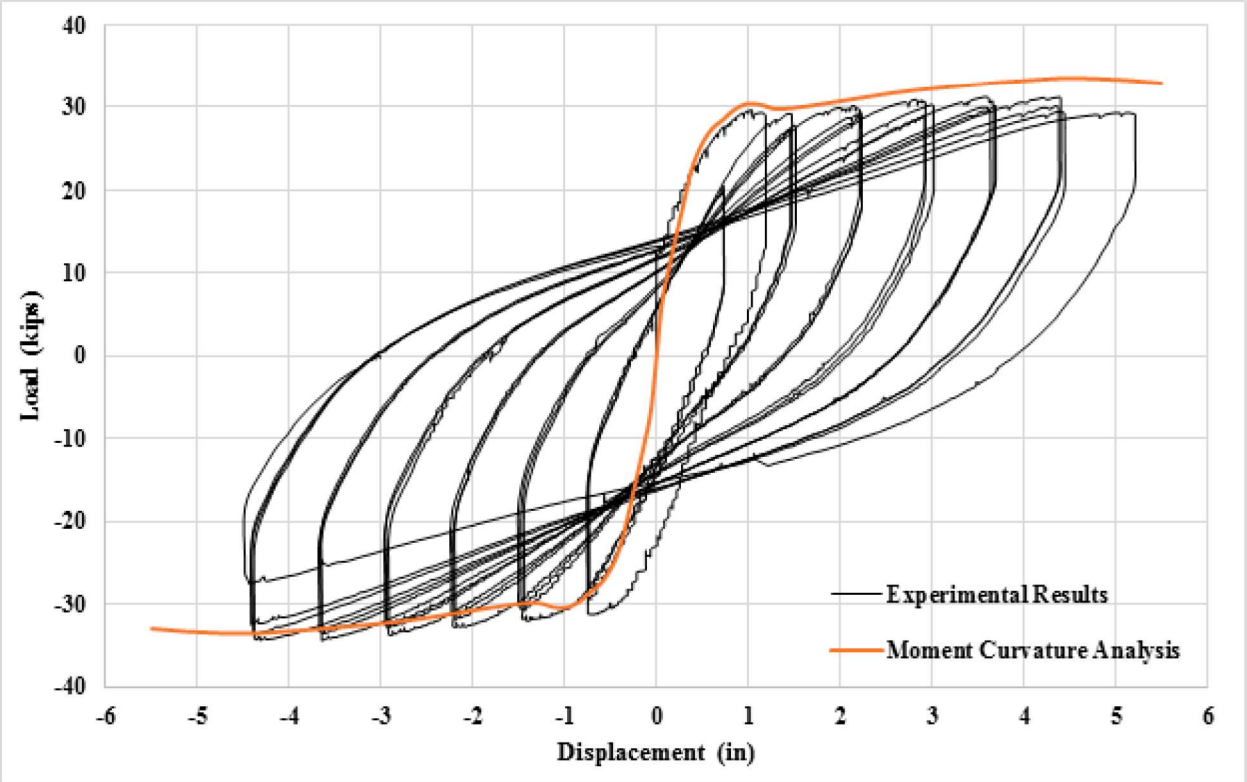


*Figure 4-14 Load-Displacement curve and moment curvature analysis.*

## 4.4. Strain Measurements

The specimen's reinforcing steel bars were instrumented with 25 strain gauges on the column longitudinal bars, cap-beam and diaphragm dowel bars, tie bars, and deck reinforcements. The strains on the columns were measured during the first 10 cycles up to first cycle of $4\Delta_y$ and the results are shown in Figure 4-15 and Figure 4-16 for south and north side of the column respectively. The strains on the dowel bars, shown in Figure 4-17 and Figure 4-18, supports the fact that the cap-beam and diaphragm remained elastic during the test. The maximum strain on these strain-gauges was 900 microstrain on the south side where the maximum strains on the column also took place. Strain measurements on the tie bars showed a gradually increase in the strains during the test with the maximum of 300 microstrain on the tie closer to the column and maximum of 200 microstrain on the further tie. Strains on the deck reinforcing steel bars were measured only after cycles of $4\Delta_y$ due to errors in data acquisition, however these strain-gauges exhibited linear relation with the lateral load with a maximum of 205 microstrain in the middle of the deck. The distribution of maximum strains on the deck in the width of specimen is shown in Figure 4-19.

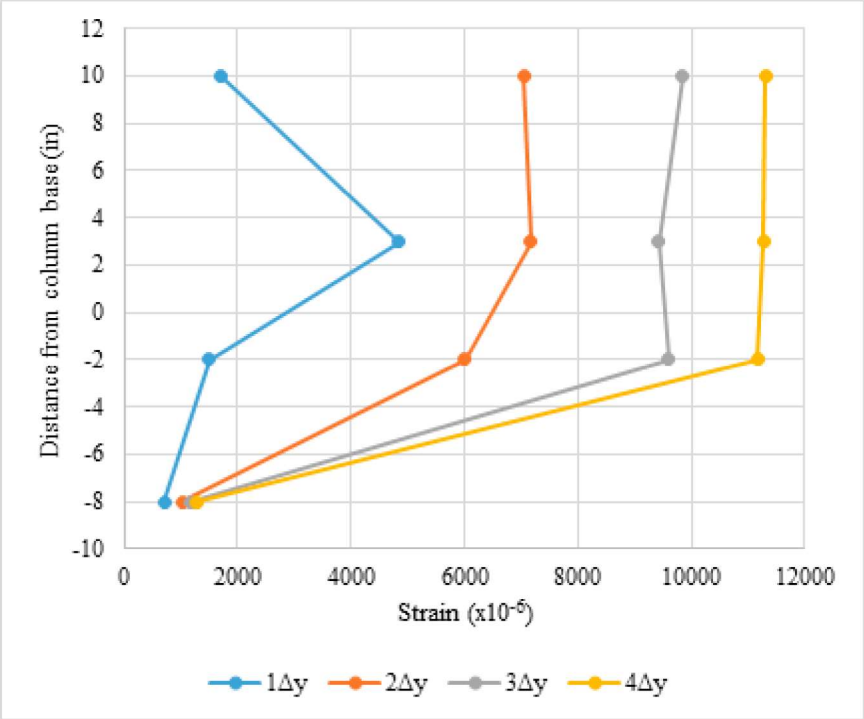


*Figure 4-15 Maximum strain on column longitudinal bar (south).*

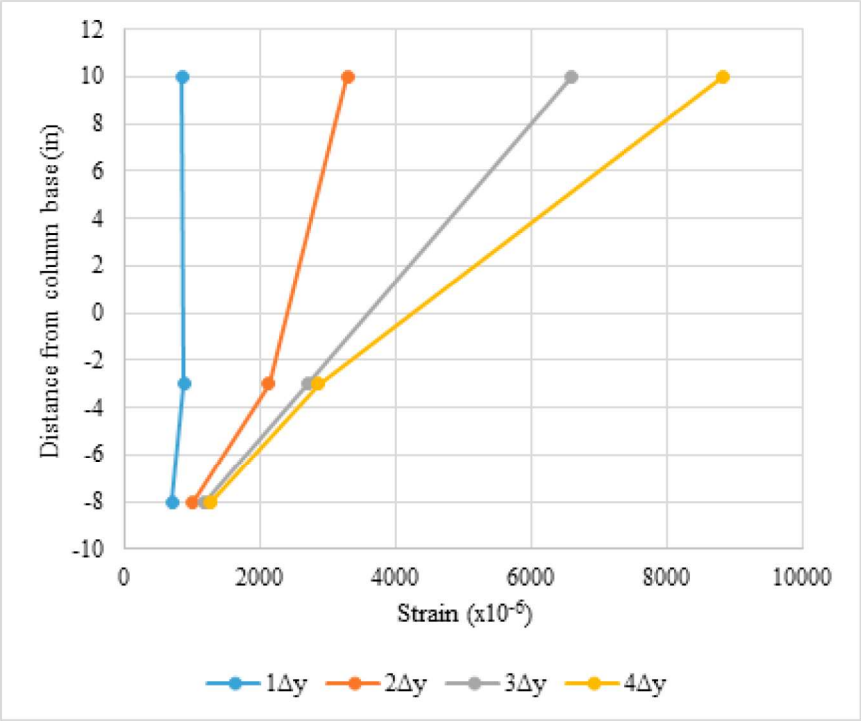


*Figure 4-16 Maximum strain on column longitudinal bar (north).*

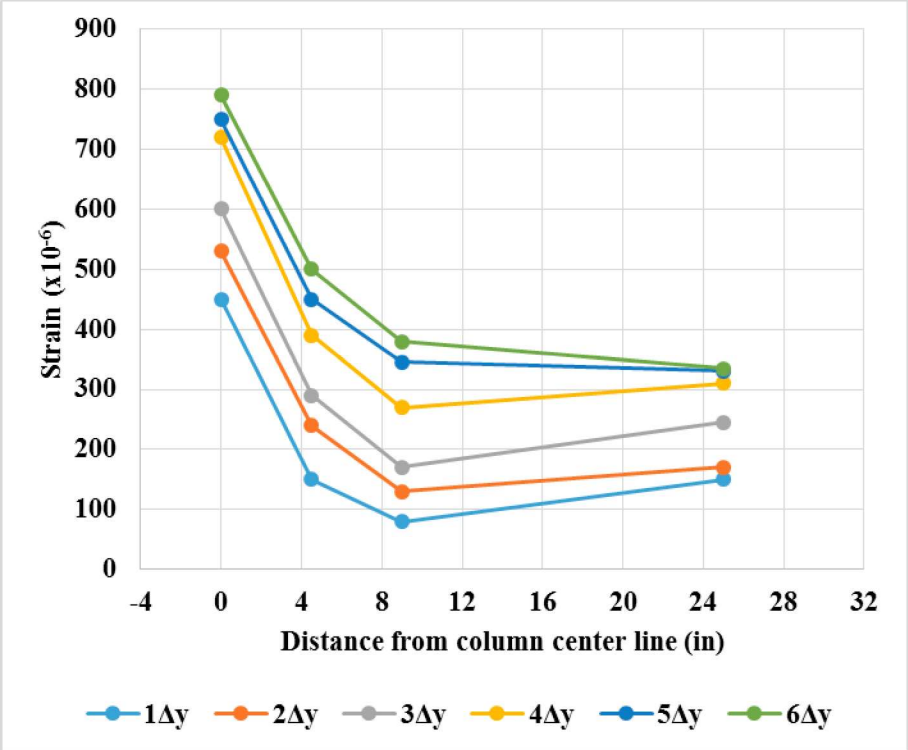


*Figure 4-17 Maximum strain in diaphragm dowel bars (north).*

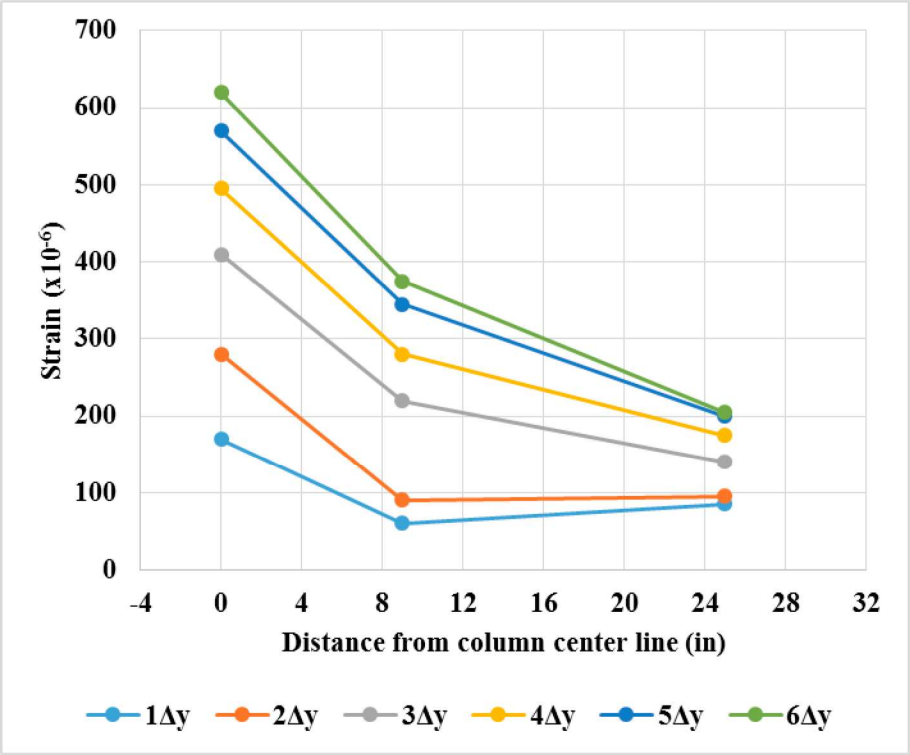


*Figure 4-18 Maximum strain in diaphragm dowel bars (south).*

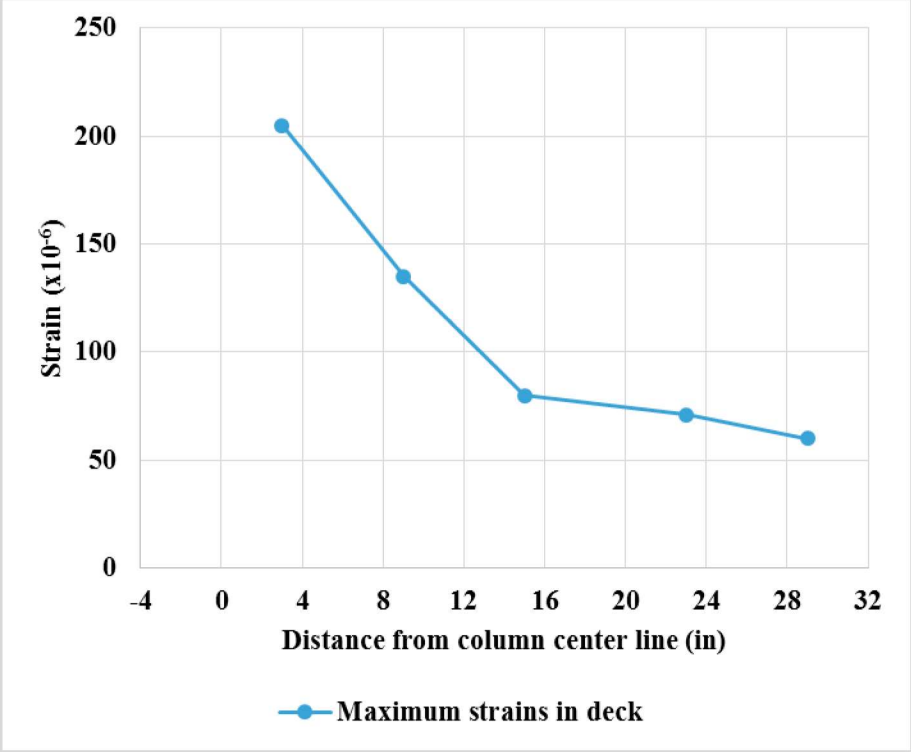


*Figure 4-19 Maximum strains in deck.*

## 4.5. Curvature and Rotation Measurements

The rotation were captured at 3 levels on the column using linear transducers. The distribution of peak curvatures along the column height is depicted in Figure 4-20. The plotted curvatures are captured from the second cycle on each increment in displacement. The results from cycles of same displacement were almost similar. The moment-rotation relation at the base of the column is shown in Figure 4-21.

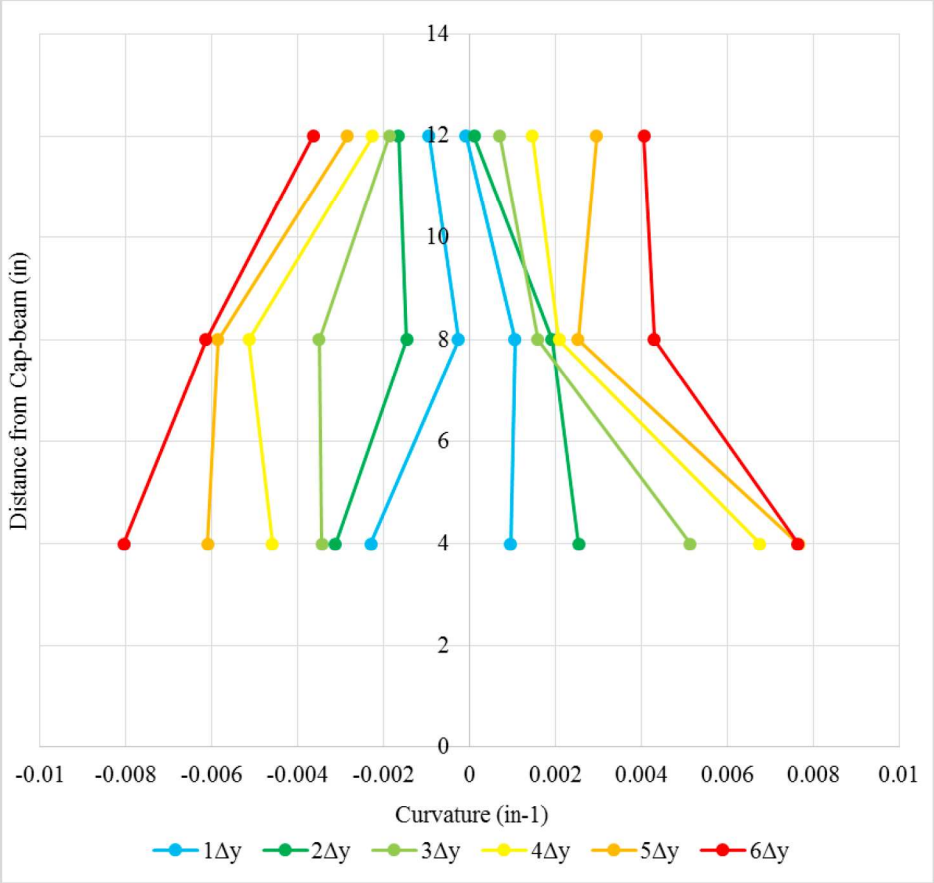


*Figure 4-20 Curvature distribution along column height.*

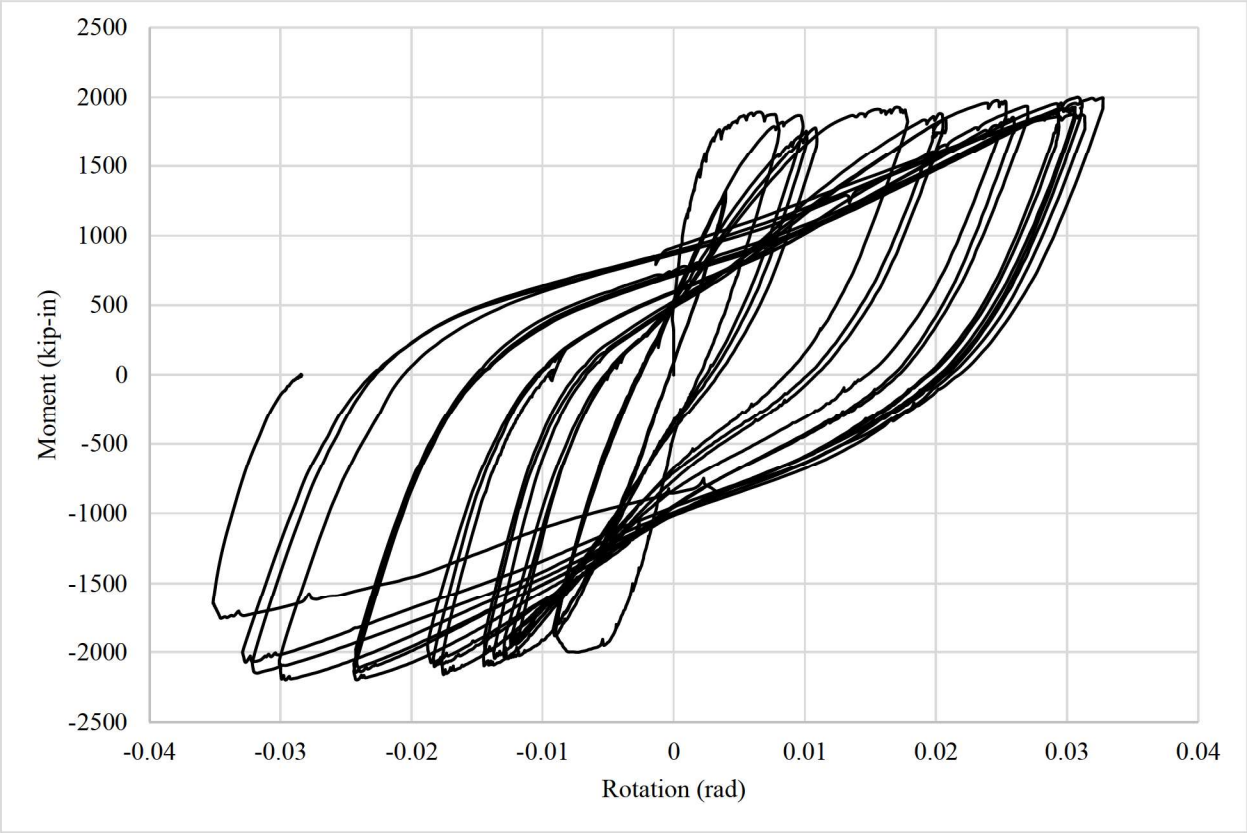


*Figure 4-21 Moment-rotation curve at bottom of the column.*

## 4.6. Discussion

The column sustained three complete cycles of $6\Delta_y$ equal to 6.6% drift ratio and bar fracture occurred at first cycle of $7\Delta_y$ (7.7% drift ratio). Therefore, the ductility capacity of column was 6 without any strength degradation observed. Strains on the column longitudinal bars developed inside the cap-beam shows the forces were distributed from column to cap-beam. Although as expected there were extensive yielding of column bars 2 inches inside the cap-beam, strains did not exceed 0.0013, 8 inches inside the cap-beam, which is low compared to yield strain of the bars (0.0023).

Based on the measured strains throughout the test, the superstructure remained elastic. The strains on the cap-beam and diaphragm dowel and tie bars had a maximum of 0.0009 and 0.0003 respectively. Stains in the deck and girders had a maximum of 0.0002. There were no visible cracks on the deck and diaphragm during the test. The only cracks on the superstructure were limited to cap-beam near the column. At higher levels of displacement some spalling on the cover of cap-beam was observed. The spalling was 1 inch deep right at the edge of column (south). Based on these observations the proposed connection of girders to cap-beam remained elastic throughout the test. Caltrans suggests to have the cap-beam at least 2 feet larger in width than the column diameter, which is 12 inch on each side. The scaling of the component test to 1/3 resulted to have

4-inch distance from column to cap-beam edge. This was the main reason of cracks and spalling in this area.

# 5. Conclusions

The component testing showed promising results for SDCL bridge system to be extended to high seismic regions. As anticipated, the plastic hinge formed at the end of the column and the connection design prevented the cap-beam (capacity protected element) from damaging. During the run of test, all monitored strains in the superstructure were exhibiting strains below yield strain which proves that the capacity protected elements remained elastic. Minor cracking was showing on the cap-beam, near the column, which is believed to be result of scaling down. However, this needs to be further investigated through parametric finite element analysis. Shake-table test on one-third scale model of the prototype bridge will be conducted in the near future and results will give a better insights of the connection in a complete bridge structure. At the conclusion of project, complete details, design and construction recommendations will be developed to extend the application of SDCL to high seismic areas.